Journal of the American Heart Association

ORIGINAL RESEARCH

Cardiospecific Overexpression of ATPGD1 (Carnosine Synthase) Increases Histidine Dipeptide Levels and Prevents Myocardial Ischemia Reperfusion Injury

Jingjing Zhao, PhD; Daniel J. Conklin, PhD; Yiru Guo, PhD; Xiang Zhang, PhD; Detlef Obal, MD, PhD; Luping Guo, MD; Ganapathy Jagatheesan, PhD; Kartik Katragadda, MD; Liqing He, PhD; Xinmin Yin, MS; Md Aminul Islam Prodhan, PhD; Jasmit Shah, PhD; David Hoetker, MS; Amit Kumar, PhD; Vijay Kumar, PhD; Michael F. Wempe, PhD; Aruni Bhatnagar, PhD; Shahid P. Baba, PhD

BACKGROUND: Myocardial ischemia reperfusion (I/R) injury is associated with complex pathophysiological changes characterized by pH imbalance, the accumulation of lipid peroxidation products acrolein and 4-hydroxy *trans*-2-nonenal, and the depletion of ATP levels. Cardioprotective interventions, designed to address individual mediators of I/R injury, have shown limited efficacy. The recently identified enzyme ATPGD1 (Carnosine Synthase), which synthesizes histidyl dipeptides such as carnosine, has the potential to counteract multiple effectors of I/R injury by buffering intracellular pH and quenching lipid peroxidation products and may protect against I/R injury.

METHODS AND RESULTS: We report here that β-alanine and carnosine feeding enhanced myocardial carnosine levels and protected the heart against I/R injury. Cardiospecific overexpression of ATPGD1 increased myocardial histidyl dipeptides levels and protected the heart from I/R injury. Isolated cardiac myocytes from ATPGD1-transgenic hearts were protected against hypoxia reoxygenation injury. The overexpression of ATPGD1 prevented the accumulation of acrolein and 4-hydroxy *trans*-2-nonenal–protein adducts in ischemic hearts and delayed acrolein or 4-hydroxy *trans*-2-nonenal–induced hypercontracture in isolated cardiac myocytes. Changes in the levels of ATP, high-energy phosphates, intracellular pH, and glycolysis during low-flow ischemia in the wild-type mice hearts were attenuated in the ATPGD1-transgenic hearts. Two natural dipeptide analogs (anserine and balenine) that can either quench aldehydes or buffer intracellular pH, but not both, failed to protect against I/R injury.

CONCLUSIONS: Either exogenous administration or enhanced endogenous formation of histidyl dipeptides prevents I/R injury by attenuating changes in intracellular pH and preventing the accumulation of lipid peroxidation derived aldehydes.

Key Words: acrolein ■ anserine ■ balenine ■ carnosine ■ carnosine synthase ■ intracellular pH ■ ischemia reperfusion

Myocardial ischemia leads to a complex series of pathological changes that involve multiple deleterious events such as a switch to anaerobic glucose metabolism and intracellular acidification and increased generation of reactive oxygen species (ROS), which initiate the formation of toxic lipid peroxidation products. If uninterrupted, these changes lead to extensive tissue injury and sustained contractile dysfunction. Therefore, the most effective intervention to rescue ischemic myocardium is timely reperfusion using thrombolytic therapy or by percutaneous coronary intervention. However, reperfusion by

Correspondence to: Shahid P. Baba, PhD, Diabetes and Obesity Center, CLB Envirome Institute, Department of Medicine, 580 South Preston Street, Delia Baxter Building, Room 421A, University of Louisville, Louisville, KY 40202. E-mail: spbaba01@louisville.edu

Supplementary Materials for this article are available at https://www.ahajournals.org/doi/suppl/10.1161/JAHA.119.015222

For Sources of Funding and Disclosures, see page 13.

JAHA is available at: www.ahajournals.org/journal/jaha

CLINICAL PERSPECTIVE

What Is New?

- This research demonstrates that enhancing myocardial production of histidyl dipeptides by cardiospecific carnosine synthase overexpression or feeding carnosine and β-alanine imparts protection from ischemia reperfusion injury.
- Decrease in intracellular pH and the accumulation of reactive aldehydes are 2 deleterious characteristics of ischemia reperfusion injury.
- Histidyl dipeptides by their dual ability to buffer intracellular pH and scavenging reactive aldehydes impart protection from ischemia reperfusion injury.

What Are the Clinical Implications?

- Histidyl dipeptides are food components found in red meat that are increased by exercise.
- Therefore, our findings lay the foundation to test the translational feasibility of these dipeptides as a prophylactic measure to prevent ischemic heart diseases.

Nonstandard Abbreviations and Acronyms

AAR	area at risk
ATPGD1	carnosine synthase
I/R	ischemia reperfusion
LFI	low-flow ischemia
ROS	reactive oxygen species

itself initiates a second cascade of complex pathological events, collectively defined as "reperfusion injury," characterized by rapid restoration of intracellular pH ($[pH]_i$), release of cardiac enzymes, mitochondrial permeability transition pore opening, and eventually cell death.[1] In the past, most therapeutic interventions to limit ischemia reperfusion (I/R) injury were designed to target a single effector (eg, antioxidants, pH buffers, or metabolic substrates),which showed only limited efficacy because preventing one aspect of I/R did not necessarily attenuate injury attributed to other contributing processes.

Multifunctional histidyl dipeptides, such as carnosine (β-alanine-histidine), have been evolutionarily conserved for at least 530 million years and are present in the muscles of families as distantly related as fish, amphibians, birds, and mammals.[2] Although the specific roles of these peptides in muscle physiology is still unclear, it is thought that by the virtue of their dissociation constant (pK_a) value, which is close to physiological pH (7.01), some of these peptides may buffer $[pH]_i$.[3] This property may be particularly useful under conditions of hypoxia, when high amounts of protons are generated by anaerobic glycolysis. However, in addition to buffering, these peptides can also quench ROS as well as reactive aldehydes such as acrolein, and 4-hydroxy-*trans*-2-nonenal (HNE),[4–6] produced during the oxidation of membrane lipids. It has also been proposed that histidyl dipeptides act as a neuromodulators or a neurotransmitters.[7] In most vertebrates, histidyl dipeptides are present in high concentrations in skeletal muscle (1–10 mmol/L) and heart (0.1–1 mmol/L) tissues,[2] in which they are locally synthesized by the enzyme ATPGD1 (carnosine synthase) from their precursors β-alanine and histidine.[8] Although the chemical properties of histidyl dipeptides are well suited to limit the effects of tissue hypoxia and I/R injury, it is unclear whether increasing the endogenous synthesis of these peptides by ATPGD1 overexpression protects against tissue injury and whether the complex I/R pathophysiology is affected by augmenting histidyl dipeptide levels.

During myocardial ischemia, the most prompt and marked change that occurs within the seconds after the onset of ischemia is cellular acidosis.[9,10] This decrease in $[pH]_i$ causes a rapid breakdown of high-energy phosphates, increases inorganic phosphates, and downregulates contraction near the ischemic zone.[9,11] In response to ischemic acidosis, H^+ ions are extruded by the Na^+-H^+ exchanger to normalize $[pH]_i$ during reperfusion, but this results in intracellular accumulation of Na^+, which in turn is exchanged for Ca^{2+} overload and the opening of the mitochondrial permeability pore.[12,13] Several Na^+-H^+ exchanger inhibitors in animal models had either resulted in modest recovery or had significant detrimental effects on I/R injury, but the clinical trials involving Na^+-H^+ exchanger inhibitors were largely negative.[14,15] In addition to acidosis, I/R generates toxic lipid peroxidation products, which accumulate in the heart even after reperfusion.[16,17] These products, particularly HNE and acrolein, can lead to coronary vasodilation[18] and decrease systolic pressure[19] and arrhythmias.[20,21] They can also deplete ATP levels, alter Na^+ and K^+ conductances, and induce cell death.[20] The contribution of these aldehydes to I/R injury is supported by extensive evidence showing that the deletion of enzymes that detoxify these aldehydes, including glutathione-*S*-transferase P,[22] aldose reductase,[23,24] and aldehyde dehydrogenase 2, increases I/R injury.[25,26] Therefore, a combinatorial strategy that could reduce acidification and prevent the accumulation of reactive aldehydes might be well suited to ameliorate concurrently several adverse factors of I/R injury.

Previous work from our laboratory and others have shown that the perfusion of isolated murine hearts by carnosine offers modest protection against I/R injury,[27,28] and intravenous injection of carnosine in rats imparts cerebroprotection.[29] Nevertheless, from these studies it is not clear whether these dipeptides act at intracellular sites or if these effects are systemic. Importantly, it is not known whether the cardioprotective effects of carnosine are related to pH buffering and/or aldehyde quenching and how it affects glucose use in the heart. In addition, in humans, histidyl dipeptides are rapidly hydrolyzed by the carnosine-specific peptidase carnosinase present in the serum, which limits its bioavailability.[30] Recent clinical trials in heart failure patients showed that carnosine feeding did not improve cardiac function, reflecting a limitation to carnosine ingestion in this setting.[31] Hence, we increased the myocardial histidyl dipeptide pool by the cardiospecific overexpression of ATPGD1. Our results showed that ATPGD1 overexpression enhances the myocardial pool of histidyl dipeptides and diminished myocardial infarct size. The results of mechanistic studies showed that both aldehyde quenching and $[pH]_i$ buffering are essential actions for optimal cardio protection by histidyl dipeptides.

METHODS

Adult male C57BL/6 mice were obtained from The Jackson Laboratory (Bar Harbor, ME). All animal protocols were reviewed and approved by the University of Louisville Institutional Animal Use and Care Committee. Detailed methodology is described in Data S1. ATPGD1-transgenic (Tg) mice were generated using the α–myosin heavy chain promoter and subjected to in vivo coronary ligation and reperfusion to induce I/R injury. Nuclear magnetic resonance (NMR) was used to quantify changes in pH in isolated perfused hearts, and metabolites were measured by liquid chromatography–mass spectrometry or gas chromatography–tandem mass spectrometry (see Data S1, and raw data will be provided on request). All of the data and methods used in the analysis and material used to conduct research will be made available at request.

Statistical Analysis

The levels of carnosine and infarct size in carnosine and β-alanine–treated and untreated mice hearts, infarct size of C57BL/6, wild type littermates (WT mice) and ATPGD1-Tg mice hearts subjected to in vivo ischemia reperfusion, and postischemic functional recovery following global ischemia in WT and ATPGD1-Tg–isolated mice hearts were analyzed by using unpaired *t* test. High-energy phosphates measured by ^{31}P NMR and ^{13}C lactate formation generated during low-flow ischemia (LFI) and reperfusion in WT and ATPGD1-Tg mice hearts were analyzed using repeated analysis of variance. Synthesis of carnosine in hearts isolated from WT and ATPGD1-Tg mice were analyzed by using the Mann-Whitney nonparametric test. Cytotoxicity of isolated cardiomyocytes isolated from WT and ATPGD1-Tg mice hearts that were subjected to normoxia and hypoxia/reperfusion and generation of aldehyde protein adducts after ischemia in the WT and ATPGD1-Tg mice hearts were analyzed by using 2-way analysis of variance followed by bonferroni test. To estimate the survival time of isolated cardiomyocytes between different treatments, 4 different models of estimating survival were evaluated as mentioned previously.[32] Fits of exponential, Weibull, linear exponential, and γ distribution to the data were estimated using a regression method for survival distribution fitting.[33] The best fits were obtained for the Weibull distribution. This distribution has been used to determine the survival in continuous carcinogenesis and isolated cardiomyocytes.[22,32,34] Survival data for cardiac myocytes were modeled using the Weibull survival distribution. Curve fitting was performed using the Proc NLIN procedure in SAS version 9.4 software (SAS Institute, Inc., Cary, NC). Two Weibull distributions were compared as described previously.[35] The number of observations "n" refers to the number of different mice hearts, and ~100 cells were counted from each mouse heart. Statistical significance was accepted at $P<0.05$. Group data are mean±SD and mean±SEM.

RESULTS

Carnosine and β-Alanine Feeding Protect the Heart From I/R Injury

To increase intracellular levels of carnosine, we placed adult male C57BL/6 mice on drinking water containing β-alanine (20 mg/mL). β-alanine is the nonproteinogenic rate-limiting amino acid that is used for carnosine synthesis. It is widely used as a food supplement to increase carnosine levels in skeletal muscle.[36,37] As shown in Figure 1A, after 7 days on β-alanine–containing water, carnosine levels were ≈7-fold higher in the hearts of treated than untreated mice (0.31±0.05 nmoles/mg protein versus 2.26±0.08 nmoles/mg protein). There was no change in anserine levels (0.0754±0.008 nmoles/mg protein versus 0.068±0.001 nmoles/mg protein; Figure S1E). To evaluate the effect of elevated myocardial carnosine levels, these mice were subjected to coronary ligation for 30 minutes followed by 24 hours of reperfusion. Heart tissues were perfused with Evans blue dye and stained with 2,3,5-triphenyl tetrazolium chloride to characterize the area at risk (AAR)

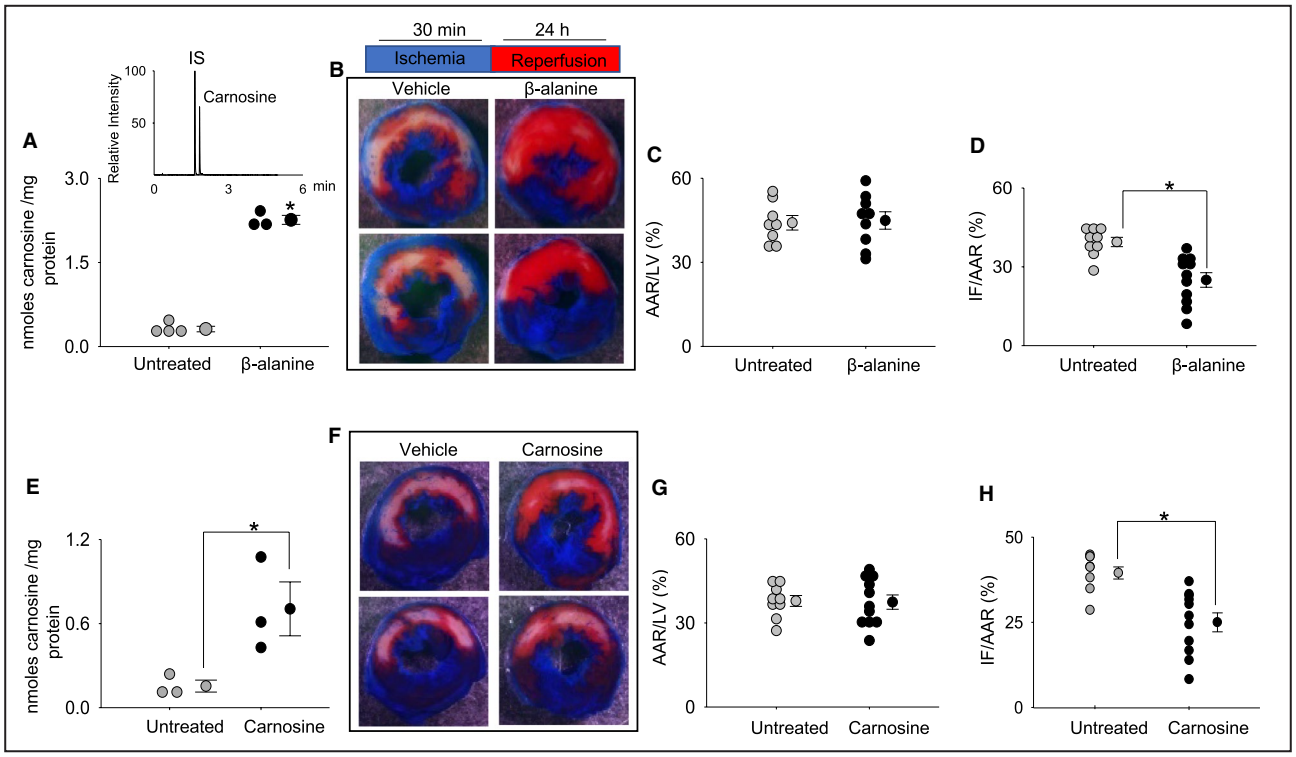

Figure 1. β-alanine and carnosine feeding protect against ischemia reperfusion injury.
A. Wild-type C57BL/6 mice were provided drinking water without (n=4) or with β-alanine (20 mg/mL; n=3) for 7 days. Myocardial carnosine levels were measured by ultra-performance liquid chromatography/tandem mass spectrometry. Inset is a representative chromatogram of carnosine and internal standard (IS) tyrosine histidine. **B**, Hearts of untreated and β-alanine–fed mice subjected to 30 minutes of ischemia followed by 24 hours of reperfusion. Representative cross-sections of 2,3,5 triphenyltetrazolium chloride staining shows the infarct zone depicted by a white area, the red area is the area at risk (AAR), and the blue region is the remote zone. (Scale bar=1 mm.) **C** and **D**, The relative ratios of the AAR to the left ventricle (LV) area and the infarct area (IF) to the AAR were compared between the untreated (n=8) and β-alanine–fed (n=9) fed mice. **E**, Mice provided drinking water with or without carnosine (10 mg/mL) for 7 days; n=3 mice in each group. **F**, Representative cross-sections of the untreated and carnosine-treated mice subjected to 30 minutes of ischemia followed by 24 hours of reperfusion. **G** and **H**, Relative ratio of AAR to the LV area and IF to the AAR were compared between the untreated (n=9) and carnosine-treated mice groups (n=11). **P*<0.05 vs the untreated mice group.

and infarct size. Figure 1B shows the representative 2,3,5-triphenyl tetrazolium chloride micrographs of the heart tissues. Quantitative analysis of Evans blue dye and 2,3,5-triphenyl tetrazolium chloride staining, indicated that the AAR/left ventricle ratio was similar between the untreated and β-alanine–treated mice (Figure 1C). However, the infarct area as a ratio of AAR was significantly lower in the β-alanine–treated than in the untreated mice (Figure 1D). To examine whether carnosine itself was as effective as its precursor, we placed the WT mice on drinking water ±10 mg/mL carnosine for 7 days, which led to a 5-fold increase in myocardial carnosine levels (0.15±0.04 nmoles/mg protein versus 0.71±0.19 nmoles/mg protein; Figure 1E). Again, there was no change in anserine levels (Figure S1F). Similar to β-alanine, carnosine feeding protected the heart from I/R damage, as reflected by a lower infarct area/AAR ratio in the hearts of the carnosine-fed mice subjected to coronary ligation and perfusion (Figure 1H). Taken together, these results suggest that increasing myocardial levels of carnosine via the delivery of carnosine or its precursor has an infarct-sparing effect. In addition, these findings strengthened the rationale for testing the role of ATPGD1, which synthesizes these dipeptides.[8]

Cardiospecific Overexpression of *ATPGD1* Protects Against I/R Injury

The enzyme ATPGD1 ligates β-alanine and histidine to form carnosine, which could be further methylated by carnosine N-methyltransferase to form anserine.[2,8,38] To examine whether the cardiospecific ATPGD1 overexpression increases myocardial levels of histidyl dipeptides, we generated the Tg mice overexpressing the mouse *ATPGD1* gene under the control of α–myosin heavy chain promoter on a C57/BL6 background. Western blot analysis confirmed that the ATPGD1 expression in the heart was increased ≈20- to 25-fold compared with the littermate non-Tg control (WT) mice (Figure 2A). Liquid chromatography–mass spectrometry measurements showed that

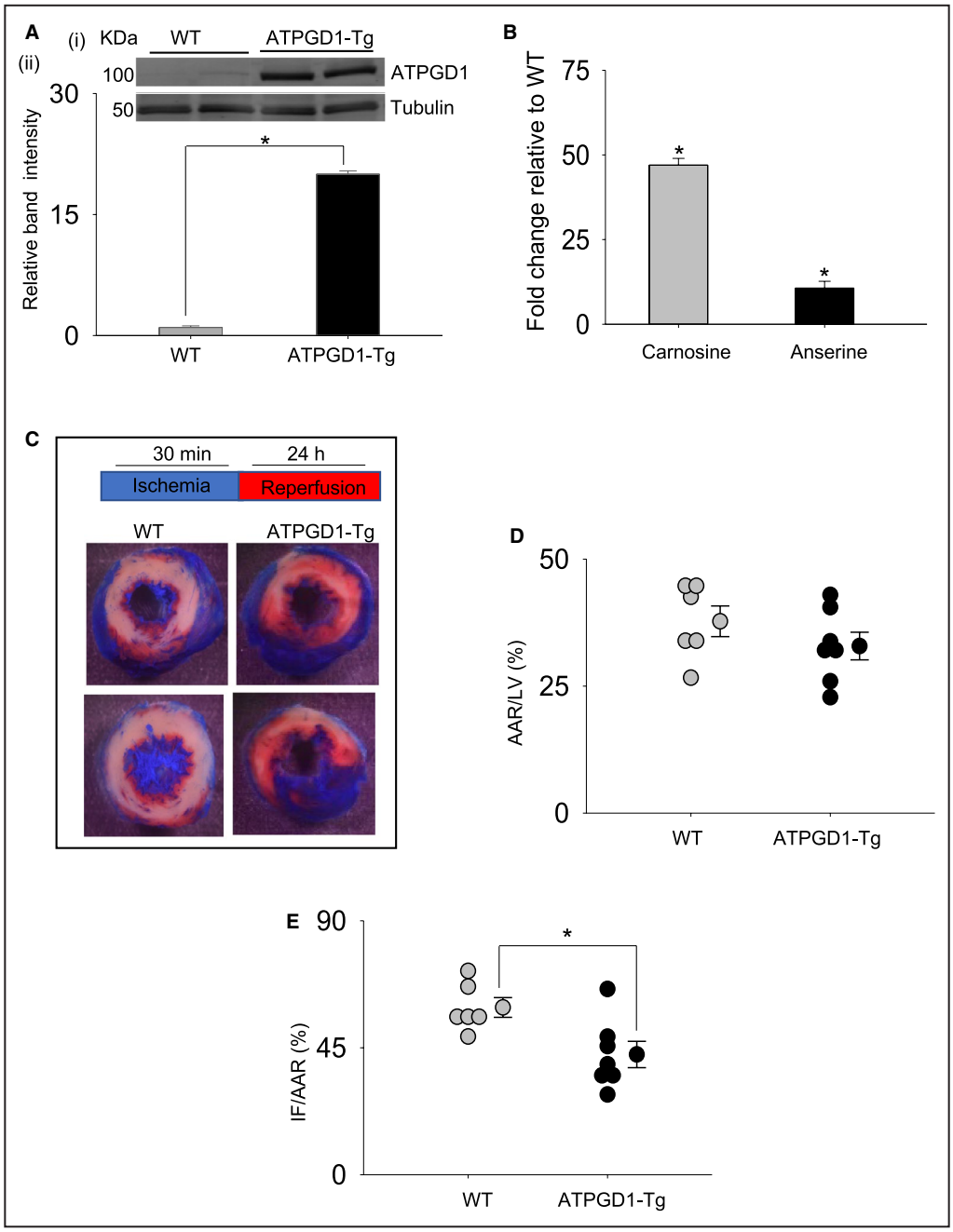

Figure 2. Cardiospecific overexpression of ATPGD1 (carnosine synthase) increases histidyl dipeptide levels and protects against ischemia reperfusion injury.
A, Representative Western blot of ATPGD1 in wild-type (WT) and ATPGD1-transgenic (Tg) hearts (**i**); lower panel represents the band intensity normalized to tubulin between the 2 groups (**ii**); n=4 in each group. **B**, Fold changes in carnosine and anserine levels in WT and ATPGD1-Tg hearts, n=4 in each group. **C**, Representative images of 2,3,5-triphenyl tetrazolium chloride–stained WT and ATPGD1-Tg hearts after 30 minutes of ischemia followed by 24 hours of reperfusion. **D** and **E**, Quantification of the ratio of area of risk (AAR) and left ventricle (LV) and the ratio of infarct size (IF) and AAR in the WT (n=6) and ATPGD1-Tg (n=7) hearts. Results are mean±SEM. **P*<0.05 vs WT mice hearts.

the carnosine and anserine levels were increased 30- to 40-fold and 10- to 12-fold, respectively, in the ATPGD1-Tg compared with the WT hearts (carnosine, WT: 0.31±0.04 nmoles/mg protein versus ATPGD1Tg: 14.57±0.39 nmoles/mg protein; anserine, WT: 0.075±0.008 nmoles/mg protein versus ATPGD1Tg: 0.791±0.137 nmoles/mg protein; Figure 2B, Figure S1A and S1B). The levels of both of these dipeptides in gastrocnemius skeletal muscle remained unchanged, attesting to the fidelity of the α–myosin heavy chain promoter (Figure S1C and S1D).

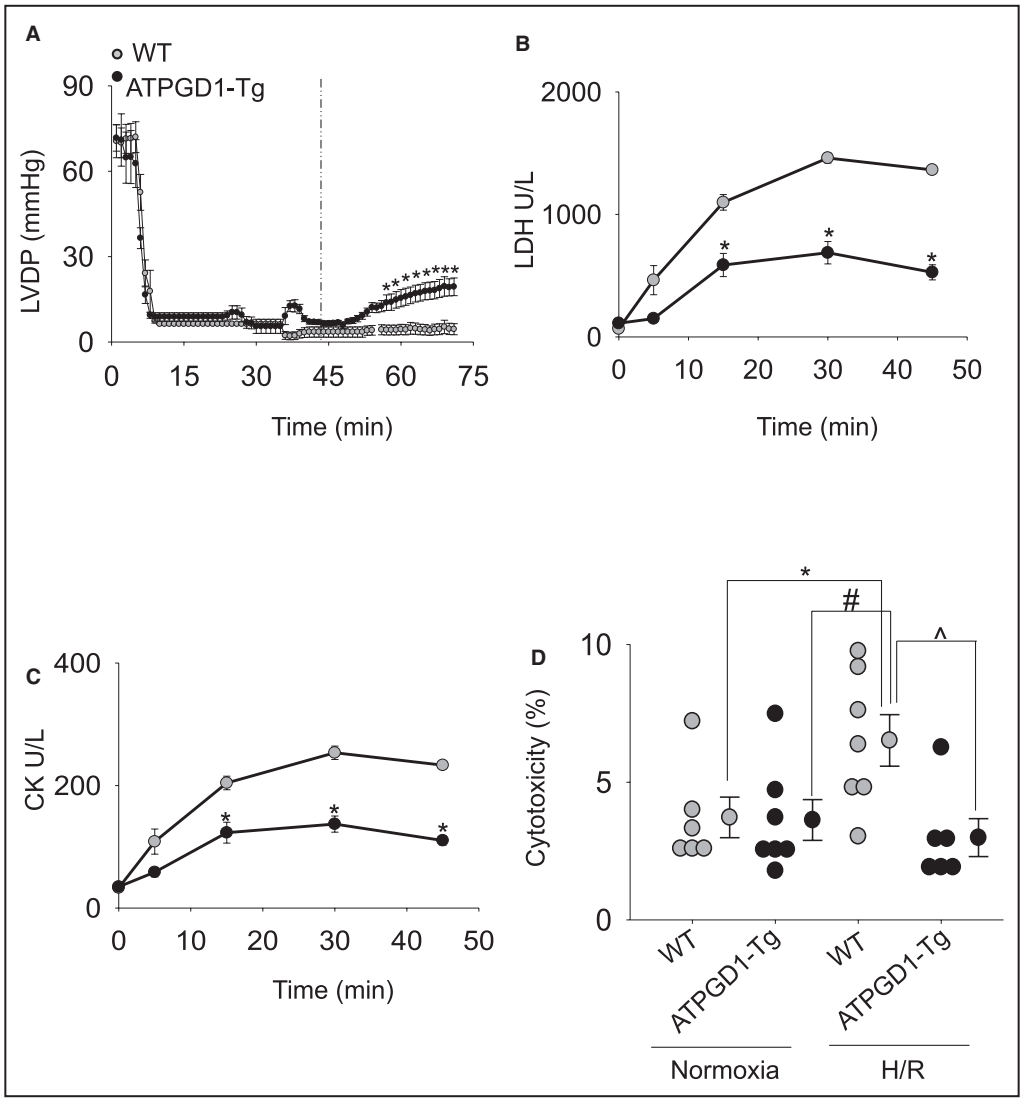

Figure 3. ATPGD1 (carnosine synthase) overexpression prevents contractile dysfunction and cardiomyocytes death.
A, Changes in the developed pressure of hearts isolated from the wild-type (WT) and ATPGD1-transgenic (Tg) mice during 10 to 12 minutes of perfusion followed by 30 minutes of ischemia and 45 minutes of reperfusion. Data are mean±SEM, n=4 mice hearts in each group; **P*<0.05 vs WT heart. **B** and **C**, Levels of lactate dehydrogenase (LDH) and creatine kinase (CK) released in the perfusate collected at different intervals of reperfusion. **D**, LDH release in the WT and ATPGD1-Tg isolated cardiomyocytes under normoxia and hypoxia/reoxygenation (H/R) conditions. Results are mean±SEM, n=6 in each group. **P*<0.05 vs WT normoxia, #*P*<0.05 vs ATPGD1-Tg normoxia, and ^*P*<0.05 vs WT H/R-treated cardiomyocytes. LVDP indicates left ventricular developed pressures.

Echocardiographic analysis showed that at baseline morphometric data and function were similar between the ATPGD1-Tg and WT mice hearts (Table S1). To determine the effect of *ATPGD1* overexpression on I/R injury, we subjected the WT and ATPGD1-Tg mice hearts to coronary ligation and reperfusion. Quantitative analysis of the 2,3,5-triphenyl tetrazolium chloride staining showed that the AAR was similar between the WT and ATPGD1-Tg mice hearts; however, the infarct size decreased significantly by ATPGD1 overexpression (Figure 2C through 2E). Taken together, these findings suggest that increasing the endogenous production of histidyl dipeptides within the heart protects from I/R injury.

ATPGD1 Overexpression Improves Postischemic Function and Protects Myocytes From Hypoxia Reoxygenation Injury

Although our results showed that carnosine protects against I/R in vivo, this could be attributed to direct effects of the dipeptide in cardiomyocytes or

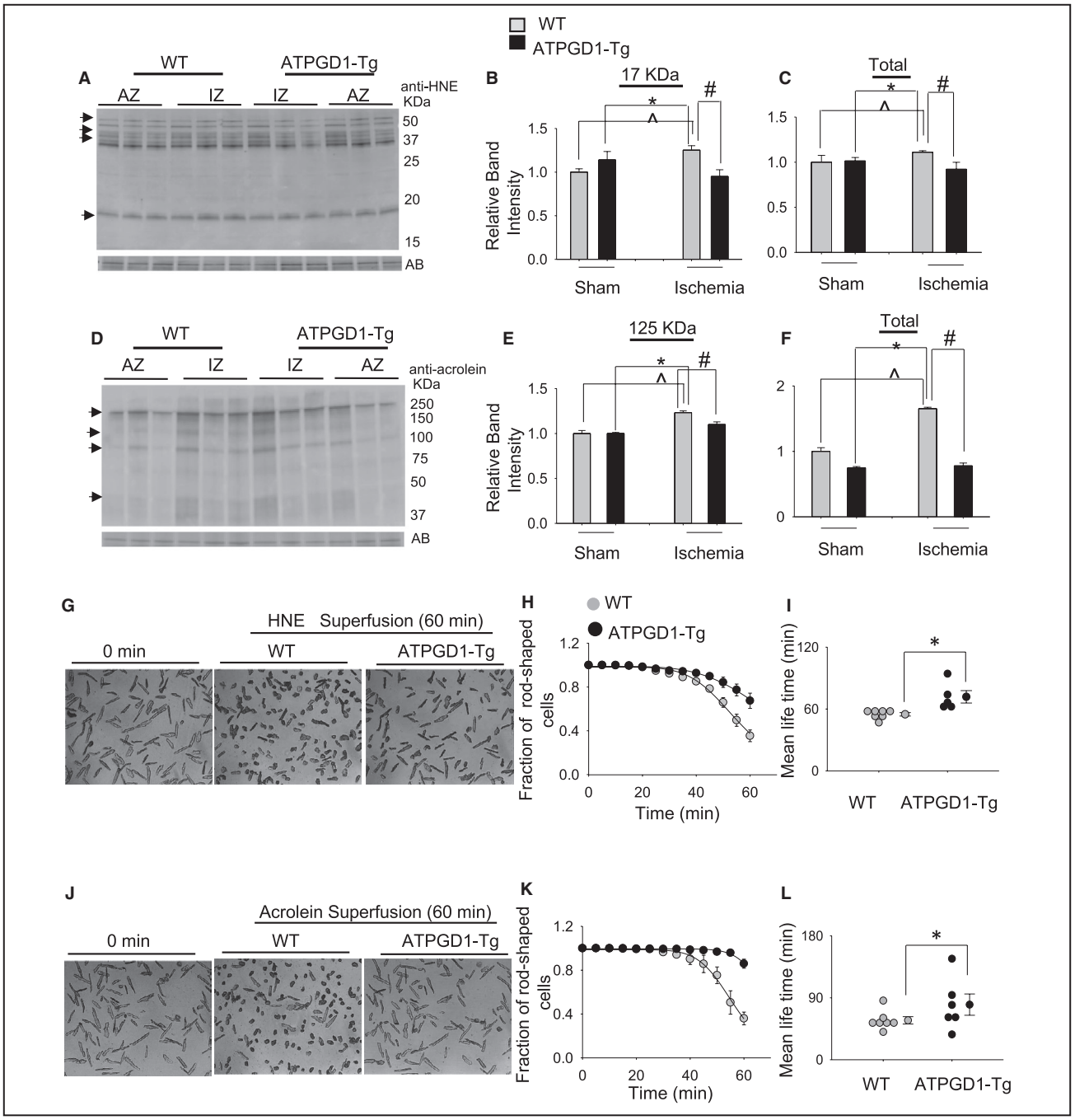

Figure 4. ATPGD1 (carnosine synthase) attenuates aldehyde accumulation and toxicity.
Representative Western blots of the wild-type (WT) and ATPGD1-transgenic (Tg) mice hearts after 30 minutes of sham and coronary ligations. The anterior zone (AZ) from sham-operated and the ischemic zone (IZ) from coronary-ligated mice hearts were developed with (**A**) anti–4-hydroxy-*trans*-2-nonenal (HNE) and (**D**) anti-acrolein antibodies and normalized with Amido-black (AB). Relative band intensities of HNE (**B** and **C**) and acrolein-modified (**E** and **F**) protein bands. Data are mean±SEM. ^*P*<0.05 vs WT sham AZ, **P*<0.05 vs ATPGD1-Tg AZ, #*P*<0.05 vs WT IZ; n=4 in each group. **G**, Representative images of adult cardiomyocytes isolated from the WT and ATPGD1-Tg hearts at 0 and 60 minutes of superfusion with HNE (50–60 μmol/L). (Scale bar=100 μmol/L.) **H**, Survival plots of cardiomyocytes isolated from WT (n=7) and ATPGD1-Tg (n=5) hearts superfused with HNE, 100 cells from each heart. Data are shown as discrete points, and the curves are best fits of a Weibull survival function. **I**, Graph showing the mean lifetime of WT and ATPGD1-Tg cardiomyocytes in the presence of HNE are presented as mean±SEM. **P*<0.05 vs WT HNE superfused cardiomyocytes. **J**, Representative images of myocytes isolated from WT and ATPGD1-Tg hearts at 0 and 60 minutes of superfusion with acrolein (5 μmol/L). (Scale bar=100 μmol/L.) **K**, Survival plots of cardiomyocytes isolated from WT (n=7) and ATPGD1-Tg (n=6) hearts superfused with HNE, 100 cells from each heart. Data are shown as discrete points and the curves are best fits of the Weibull survival function. **L**, Graph showing the mean lifetime of WT and ATPGD-Tg cardiomyocytes. **P*<0.05 vs WT acrolein-treated myocytes.

neurohormonal and inflammatory responses triggered by coronary occlusion and reperfusion. Hence, to exclude neurohormonal and inflammatory responses, we perfused isolated WT and ATPGD1-Tg mice hearts in the Langendorff mode for 10 to 12 minutes and then subjected them to 30 minutes of global ischemia followed by 45 minutes of reperfusion. At baseline, the left ventricular developed pressures were comparable between the WT and ATPGD1-Tg hearts; however, during reperfusion, the ATPGD1-Tg hearts had improved systolic functional recovery, as demonstrated by higher left ventricular developed pressures compared with the WT mice hearts (Figure 3A). Similarly, the release of the myocardial enzymes lactate dehydrogenase and creatine kinase was less in the ATPGD1-Tg than in the WT hearts, indicating the cardiospecific protection attributed to ATPGD1 overexpression (Figure 3B and 3C).

To localize further the site of action of ATPGD1, we isolated the cardiac myocytes from the WT and ATPGD1-Tg mice hearts and subjected them to either normoxia (5 hours) or hypoxia (3 hours) followed by 2 hours of reoxygenation. The WT cardiac myocytes subjected to hypoxia and reoxygenation showed greater lactate dehydrogenase release than normoxic cardiac myocytes; however, the lactate dehydrogenase release in myocytes from the ATPGD1-Tg hearts subjected to hypoxia and reoxygenation was similar to that from normoxic WT cells, and significantly lower than the WT myocytes subjected to hypoxia and reoxygenation (Figure 3D). Collectively, these data indicate that increased intracellular levels of carnosine protect myocytes from the deleterious effects of hypoxia and reoxygenation.

ATPGD1 Overexpression Prevents Aldehyde Accumulation in Ischemic Hearts and Protects Aldehyde Toxicity

Given our findings that ATPGD1-Tg mice hearts are protected from I/R injury, we next determined the mechanism by which *ATPGD1* overexpression affects the heart during ischemia. For this, we subjected the WT and ATPGD1-Tg mice hearts to 40 minutes of coronary ligation in vivo and analyzed the ischemic zone of the ligated hearts and the anterior zone of the sham-operated hearts for protein-HNE and protein-acrolein adducts by Western blotting. Our results showed that the protein-HNE adducts were more abundant in the ischemic zone of the WT ischemic hearts than in the anterior zone of the sham-operated WT and ATPGD1 hearts. Importantly, the accumulation of the protein-HNE adducts was mitigated in the ischemic zone of the ATPGD1-Tg mice hearts (Figure 4A through 4C). Moreover, less protein-acrolein adducts accumulated in the ischemic zone of ATPGD1-Tg ischemic hearts (Figure 4D through 4F). These observations are consistent with the notion that elevated levels of carnosine decreases the accumulation of lipid peroxidation–derived aldehydes in the ischemic hearts.

Given that aldehyde protein-adduct accumulation was diminished in the ATPGD1-Tg ischemic hearts, we next tested whether ATPGD1 overexpression would protect against aldehyde toxicity. Previous work has shown that these aldehydes induce myocyte hypercontracture.[20,21] Therefore, we perfused myocytes isolated from the WT and ATPGD1-Tg hearts with HNE for 60 minutes, continuously monitored their shape under a light microscope, and calculated cell survival using the Weibull distribution function. These analyses showed that although HNE perfusion caused hypercontracture in both WT and ATPGD1-Tg cardiac myocytes, the mean lifetime of WT myocytes was 55±2 minutes, whereas the ATPGD-1-Tg survived with a mean lifetime of 72±6 minutes (Figure 4G through 4I). The ATPGD1-Tg cardiac myocytes were also resistant to acrolein-induced hypercontracture. The mean lifetime of WT cardiomyocytes superfused with acrolein was 55±2 minutes, which was less than that of ATPGD1-Tg myocytes (72±5 minutes; Figure 4J through 4L). Collectively, these results suggest that high intracellular levels of carnosine protect against the toxicity of a structurally diverse range of aldehydes generated by lipid peroxidation.

ATPGD1 Overexpression Prevents Ischemic Changes in $[pH]_i$ and High-Energy Phosphate Content

Given that ATPGD1 overexpression enhanced myocardial histidyl dipeptide levels, which can buffer pH,[2] we next tested whether it could also preserve change in $[pH]_i$ during myocardial I/R. For this, we used ^{31}P NMR spectroscopy to measure the changes in myocardial ATP, phosphocreatine (PCr), and $[pH]_i$ during I/R. Hearts isolated from the WT and ATPGD1-Tg mice were subjected to 20 minutes of perfusion, followed by 20 minutes of LFI (10% of baseline) and 50 minutes of reperfusion. Figure 5A and 5D shows the representative ^{31}P NMR spectra at baseline, LFI, and reperfusion of the WT and ATPGD1-Tg isolated hearts, respectively**.** From the left to right, the peaks present inorganic phosphate; PCr; and γ, α, and β phosphates of ATP; and the area under the curve of respective resonances were used to calculate the amount of each metabolite. The baseline spectra of PCr was similar between the WT and ATPGD1-Tg hearts, which was reduced to ~50% of baseline in both the WT and ATPGD1-Tg hearts during LFI; however, the decrease was slightly less pronounced in the ATPGD1-Tg hearts. During reperfusion, the PCr recovery in the WT hearts was nearly 100%; however, in the ATPGD1-Tg hearts, the PCr recovery exceeded

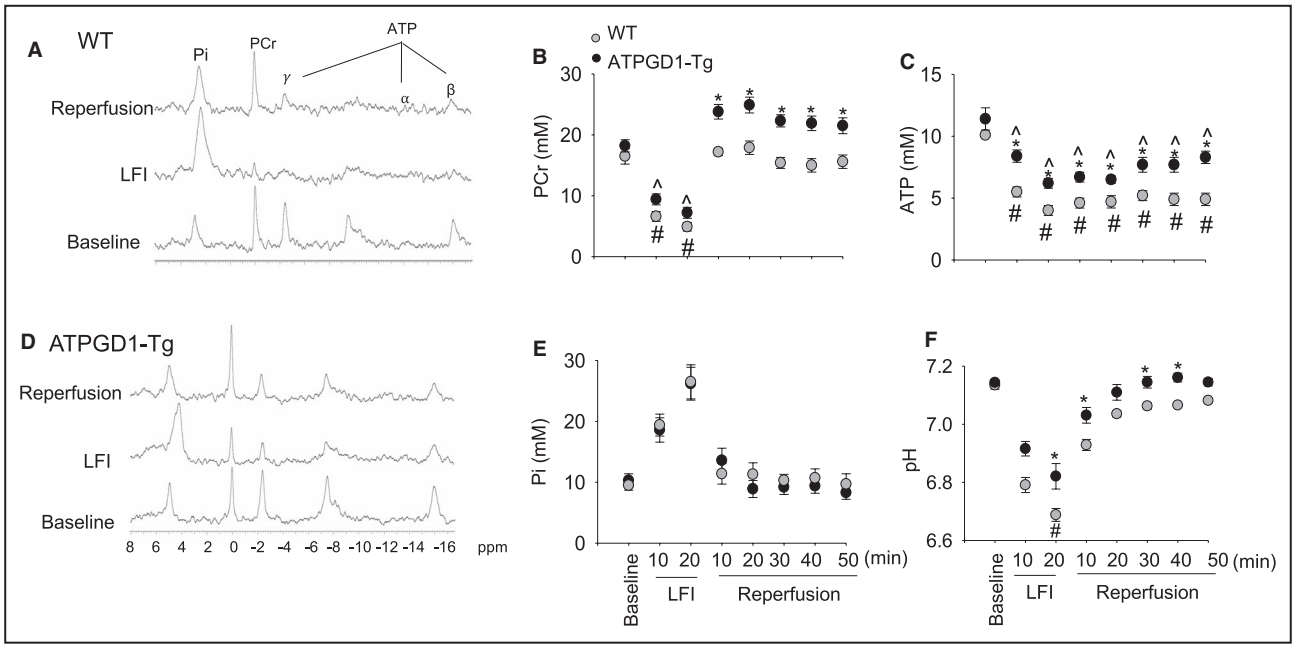

Figure 5. ATPGD1 (carnosine synthase) overexpression enhances buffering capacity during ischemia reperfusion injury. Representative ^{31}P NMR spectra from wild-type (WT) (**A**) and ATPGD1-transgenic (Tg) (**D**) hearts during baseline, low-flow ischemia (LFI), and reperfusion. Pi, PCr, γ, α, β denotes inorganic phosphate, phosphocreatine, and resonances of ATP, respectively. Changes in PCr (**B**), ATP (**C**), Pi (**E**), and pH (**F**) during baseline, LFI, and reperfusion. Data are mean±SEM; n=6 mice in each group. *P<0.05 vs WT, #P<0.05 vs WT baseline, and ^P<0.05 vs ATPGD-Tg baseline.

the baseline levels and remained higher than in WT hearts throughout the reperfusion (Figure 5B). Basal ATP levels were similar between the WT and the ATPGD1-Tg hearts, and LFI resulted in a 40% to 50% decrease in ATP levels in the WT hearts, which did not recover during reperfusion. In contrast, the ATP levels in the ATPGD1-Tg hearts decreased to only 30% to 40% of the baseline during LFI and remained higher than in the WT hearts (Figure 5C). The inorganic phosphate increased substantially in both the WT and ATPGD1-Tg hearts during LFI and reached preischemic levels during reperfusion in both groups (Figure 5E). These results suggest that increasing the abundance of carnosine in the heart prevents the loss of high-energy phosphates during ischemia and promotes their restoration during reperfusion.

At baseline, $[pH]_i$ was similar between the WT and ATPGD1-Tg hearts (7.13±0.04 versus 7.14±0.01), but in WT hearts, $[pH]_i$ fell rapidly by 0.34±0.02 pH units after 10 minutes and 0.45±0.02 pH units after 20 minutes of LFI. In contrast, there was less acidosis in the ATPGD1-Tg hearts. In these hearts, the mean fall of $[pH]_i$ was 0.23±0.02 units after 10 minutes and 0.32±0.03 units after 20 minutes of LFI. During the first 10 minutes of reperfusion, the $[pH]_i$ in the WT hearts reached 6.92±0.01 and thus had recovered 0.21±0.01 pH units. However, in the ATPGD1-Tg hearts, the $[pH]_i$ reached 7.03±0.01, suggesting a greater recovery of $[pH]_i$ compared with the WT hearts. The rates of $[pH]_i$ recovery during 20 to 50 minutes of reperfusion was delayed in the WT hearts and did not reach preischemic levels, whereas the $[pH]_i$ in the ATPGD1-Tg hearts after 30 to 40 minutes of reperfusion was similar to baseline (7.08±0.01 versus 7.13±0.01; Figure 5F). Taken together, these results provide direct evidence that ATPGD1 overexpression augments intracellular buffering and mitigates acidosis during I/R.

Both Buffering and Aldehyde Quenching Are Essential for Cardiac Protection by Histidyl Dipeptides

Because ATPGD1 overexpression seems to protect against carbonyl stress and $[pH]_i$ imbalance, we next examined which of these properties might be essential for cardioprotection. To test the relative contribution of aldehyde quenching and buffering, we synthesized the natural carnosine analog anserine, which is methylated at the N^{π} residue of histidine and has aldehyde-binding capacity similar to carnosine (Figure S2).[39] However, in comparison with carnosine, anserine has a lower buffering capacity (pKa 7.15).[40] In addition, we also synthesized balenine, which is methylated at the N^{τ} residue of histidine, and therefore has a higher buffering (pKa 6.93), yet lower aldehyde binding, capacity than does carnosine.[21,40] Thus, unlike carnosine, balenine does not protect cardiomyocytes against aldehyde-induced hypercontracture.[21] To determine how the differential biochemical properties of these

dipeptides influences I/R injury, we perfused isolated C57/BL6 mice hearts with either anserine or balenine (1 mmol/L) and subjected these hearts to I/R as previously. The results of these experiments showed that neither balenine nor anserine was able to improve the recovery of postischemic contractile function (Figure 6A and 6B). The release of cardiac enzymes (creatine kinase and lactate dehydrogenase) in balenine-perfused and anserine-perfused hearts was similar in magnitude to their release in untreated WT hearts (Figure 6C through 6F). From these results, we infer that the loss of either the buffering capacity or aldehyde binding abolishes the cardioprotective effects of histidyl dipeptides, and therefore both of these properties are essential for the cardioprotective effects of carnosine.

ATPGD1 Overexpression Preserves Intermediary Metabolism During Ischemia

Extensive evidence suggests that elevated glucose levels could be beneficial to improve recovery from I/R

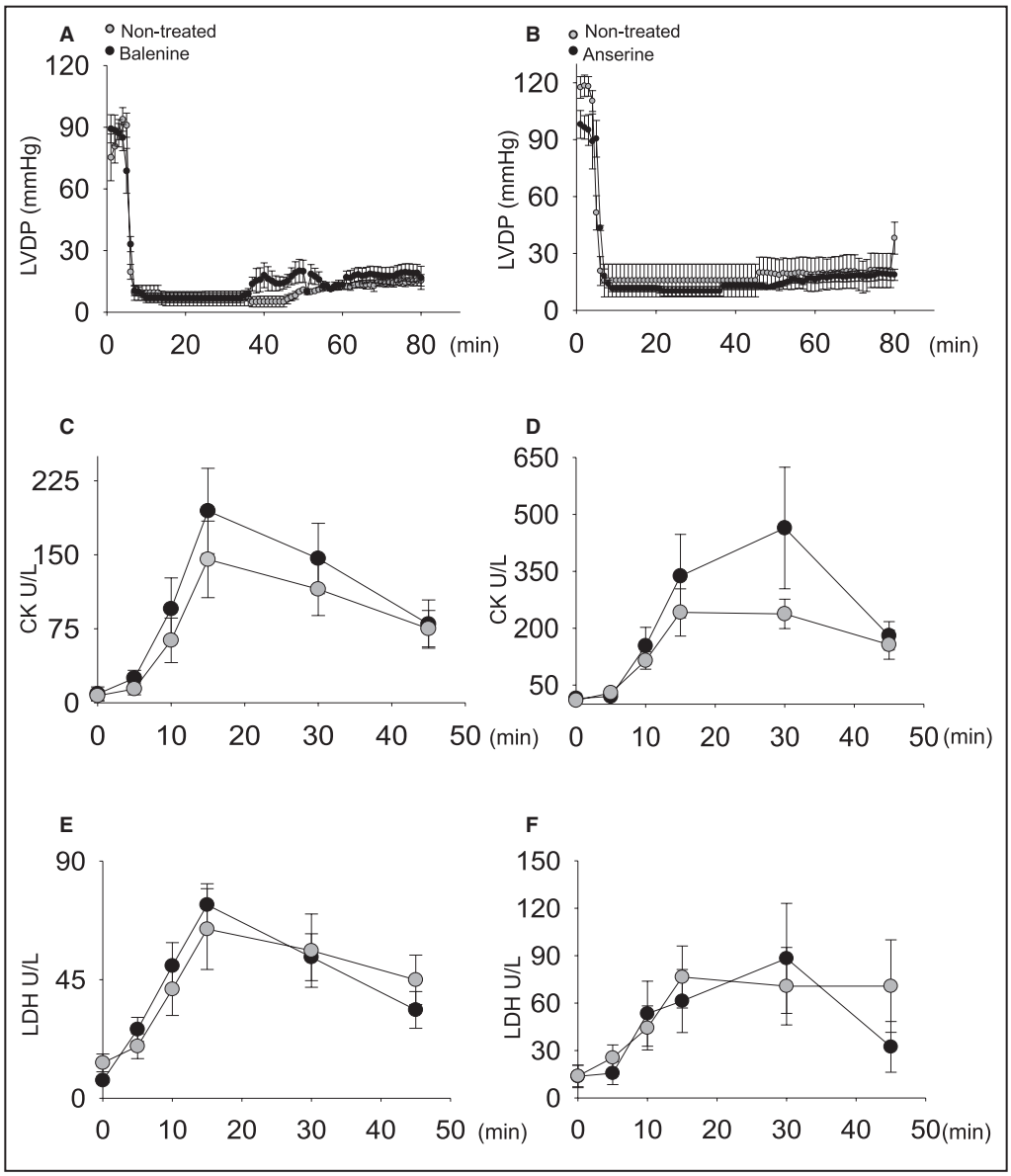

Figure 6. Histidyl dipeptide analogs balenine and anserine were unable to restore the contractile function.

Changes in the developed pressure of C57BL/6 mice hearts perfused with (**A**) balenine and (**B**) anserine followed by 30 minutes of ischemia and 45 minutes of reperfusion. Data are mean±SEM; n=4 mice hearts in each group. **P*<0.5 vs wild-type heart. Levels of creatine kinase (CK) (**C** and **D**) and lactate dehydrogenase (LDH) (**E** and **F**) released in the perfusate collected at different intervals of reperfusion. LVDP indicates left ventricular developed pressures.

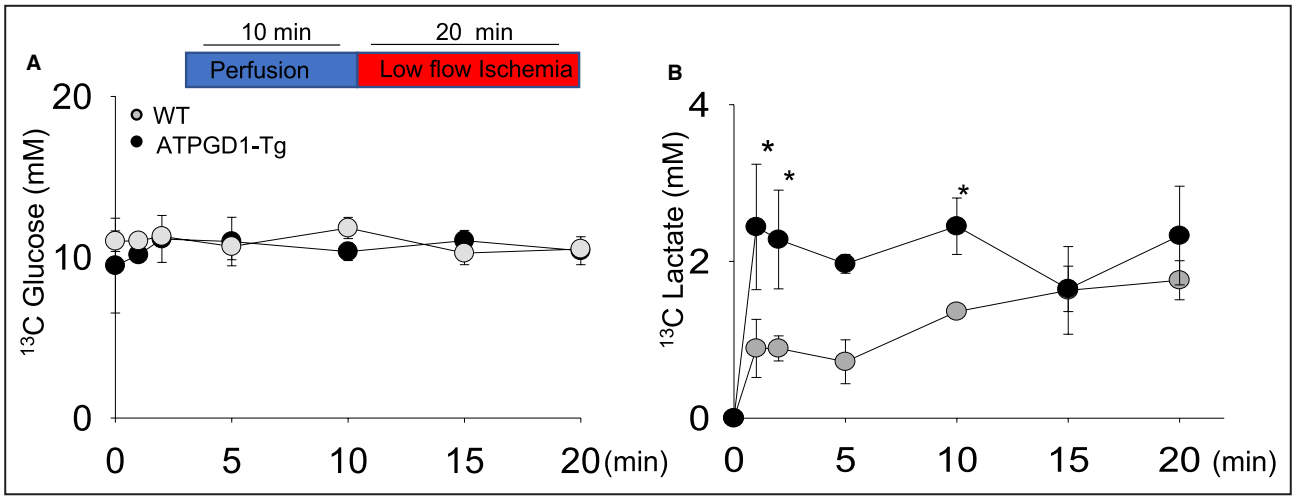

Figure 7. Anaerobic glycolysis is increased in carnosine synthase-transgenic (Tg) ischemic hearts.
A, Wild-type (WT) and ATPGD1-Tg isolated hearts were perfused for 10 minutes with ^{13}C D-glucose in the Langendorff mode, followed by 20 minutes of low flow ischemia. Levels of (**A**) ^{13}C D-glucose and (**B**) ^{13}C-lactate in perfusates collected at different time intervals. Data are mean±SEM; n=5 mice in each group. *P<0.05 vs WT heart. ATPGD1 indicates carnosine synthase.

injury.[41–43] Our results so far suggested that ATPGD1 overexpression prevents intracellular acidification during ischemia. Although it has been proposed that carnosine promotes glycolysis by buffering pH,[2] direct evidence for such a proglycolytic effect is lacking. To examine whether ATPGD1 overexpression affects glycolysis, we perfused isolated WT and ATPGD1-Tg hearts with^{13}C glucose for 10 minutes followed by 20 minutes of LFI. Perfusates from these hearts were collected at different times and analyzed for^{13}C glucose and^{13}C lactate by liquid chromatography–mass spectrometry. We found that the^{13}C glucose levels measured at different time points of LFI were similar between the WT and ATPGD1-Tg hearts. However,^{13}C lactate formation during 1, 2, and 10 minutes of LFI was higher in the perfusates of the ATPGD1-Tg rather than the WT hearts (Figure 6B and 7A). Taken together, these results suggest that despite the similar levels of glucose uptake, ATPGD1 overexpression increases glucose use under ischemic conditions, presumably by increasing the rates of glycolysis by buffering $[pH]_i$.

DISCUSSION

The major findings of this study are that cardiac myocyte–restricted overexpression of ATPGD1 enhances myocardial production of carnosine and thereby protects the heart from I/R injury. In addition, augmenting myocardial carnosine levels by β-alanine or carnosine supplementation also imparts cardioprotection. Our results show that ATPGD1 overexpression decreased the formation of protein-aldehyde adducts in the ischemic heart and diminished the toxicity of lipid peroxidation products. We also found that the overexpression of ATPGD1 attenuated I/R-induced changes in $[pH]_i$ and intermediary metabolism that accompany myocardial I/R. The protective effects of carnosine were not duplicated by the structurally related histidyl dipeptides anserine and balenine, suggesting that the multifunctional chemistry of carnosine is essential for cardioprotection. Taken together, these findings for the first time reveal a direct cardioprotective role of ATPGD1 and uncover new aspects of cardioprotection against myocardial ischemic injury targeted by ATPGD1-synthesized dipeptides. Given that ATPGD1 synthesizes multifaceted dipeptides, which are readily hydrolyzed in human serum diminishing its bioavailability, these results suggest that modulating the endogenous production via ATPGD1 overexpression may be a key strategy to prevent and attenuate myocardial I/R injury and related pathological conditions in humans.

Carnosine, anserine, and balenine are evolutionarily conserved dipeptides that are present in a high abundance in energetically active tissues such as the striated muscles and neurons.[2] Among these dipeptides, carnosine is widely present in the humans, whereas anserine and balenine are mostly found at relatively higher levels in birds and whales, respectively.[40] In this study, we found that the mouse heart contains 300 to 350 nmoles/g protein of carnosine and 75 to 80 nmoles/g protein of anserine, which are consistent with the expected distribution of these peptides in mammalian hearts. Nevertheless, despite their near ubiquitous distribution, the physiological role of these peptides is understudied, and it is unclear what specific function they perform in different tissues. Most previous studies on histidyl dipeptides has focused on their potential ability to increase exercise capacity, and β-alanine is frequently ingested by professional athletes

as a performance-enhancing supplement. The skeletal muscle levels of carnosine are increased by high-intensity exercise, suggesting that it plays an important role in skeletal muscle physiology.[36] Although the specific mechanisms by which carnosine increases exercise capacity remain unknown. It is widely believed that it can enhance exercise performance by buffering $[pH]_i$ and thereby preserve glycolysis during hypoxia[36,44,45]; however, direct evidence regarding the proglycolytic effects is lacking.

In addition to buffering pH, carnosine can also react with a variety of electrophiles, such as the reactive aldehydes generated by lipid peroxidation. Indeed, in our previous work we found that carnosine reacts directly with HNE and acrolein and that the resultant conjugates are metabolized and excreted in mouse and human urine.[27] Therefore, carnosine may be an endogenous antioxidant that removes reactive aldehyde species, acting in parallel to glutathione-linked detoxification. This notion is supported by our recent observation that an increase in carnosine levels attributed to β-alanine supplementation results in increased scavenging of lipid peroxidation products in human skeletal muscle, generated during high-intensity exercise.[36] Carnosine treatment has also been reported to protect the brain from ischemic damage,[29] and topical administration of carnosine accelerates wound healing in *db/db* mice.[46] Carnosine perfusion in isolated hearts has also been shown to marginally improve functional recovery of isolated ischemic rat and mice hearts.[27,28,47] Nonetheless, the mechanisms underlying the cardioprotective effects of carnosine remain unknown, and it is unclear whether carnosine protects by targeting extracellular sites or intracellular pathology and which cell types in the heart are targeted. Therefore, we generated ATPGD1-Tg mice to selectively increase carnosine levels within cardiomyocytes, and we undertook a comprehensive evaluation of the mechanisms of carnosine-mediated cardioprotection.

We found that the cardiospecific overexpression of ATPGD1 reduced the infarct size both in vivo and ex vivo and that cardiac myocytes overexpressing ATPDGD1 were resistant to hypoxia reoxygenation injury. Although cardiospecific ATPGD1 overexpression enhanced the myocardial levels of histidyl dipeptides 40- to 50-fold and mice fed with β-alanine and carnosine enhanced the myocardial carnosine levels 4- to 7-fold, both treatments had similar infarct-sparing effects, suggesting that physiological dosing of β-alanine and carnosine could be cardioprotective. Together these observations provide unequivocal evidence that carnosine protects the heart by targeting sites and events within cardiac myocytes, without directly affecting extracellular events, neurohormonal changes, or even inflammatory responses that accompany myocardial I/R.

Previous work has shown that myocardial ischemia is associated with acidification and a decrease in ATP levels attributed to the progressive failure of glucose and fatty acid metabolism. Myocardial ischemia also creates conditions that promote ROS generation, which exacerbates tissue injury and induces cell death. However, the relationship between acidification and loss of ATP is unclear, and the contribution of these changes to the ROS generation has not been clarified. Moreover, it is unclear to which extent ROS themselves or the secondary products they generate mediate tissue injury. Although free radicals and ROS are highly reactive, they are short lived and therefore much of their injury has been attributed to their secondary, more stable, products, such as the aldehydes generated by lipid peroxidation.[48,49] Several studies have shown that lipid peroxidation–derived aldehydes accumulate in cardiac tissue within 5 to 10 minutes of ischemia and that these aldehydes propagate the I/R injury.[16,22,50] Of the several reactive aldehydes generated during I/R, HNE and acrolein are the most potent and toxic species that promote ischemic injury.[51–53] Given the extensive evidence linking reactive aldehydes to tissue injury, we investigated whether increasing myocyte levels of carnosine protects the heart by detoxifying lipid peroxidation products. We found that ATPGD1 overexpression decreased the accumulation of protein-HNE and protein-acrolein adducts in the heart and that myocytes isolated from the ATPGD1-Tg heart were resistant to HNE and acrolein-induced hypercontracture. When taken together, these observations support the notion that the cardioprotective effects of high carnosine levels may be related to a greater antioxidant capacity of myocytes, specifically their greater ability to detoxify the toxic products of lipid peroxidation.

In addition to preventing oxidative injury, carnosine could also protect the heart by buffering changes in $[pH]_i$. Because of its histidyl group, carnosine is an efficient buffer with a pKa value near $[pH]_i$.[40] Previous studies with racehorses and greyhound dogs as well as elite human sprinters have shown that high levels of histidyl dipeptides can increase the intracellular buffering capacity of skeletal muscle.[54,55] Moreover, it has been recently suggested that the buffering potential of the heart, augmented by exercise, might be associated with an increase in the cardiac pool of histidyl dipeptides.[56,57] Changes in $[pH]_i$ are an important aspect of I/R injury. Extensive data have shown that acidification during I/R promotes cardiac injury by affecting cardiac metabolism and mechanics.[58–60] Because carnosine has been shown to act as a mobile buffer that regulates the Ca^{2+} and H^+ signaling in isolated cardiac myocytes,[61] it seems that intracellular buffering may be important aspect of its cardioprotective properties. Indeed, we found that although ATPGD1 overexpression did not affect basal $[pH]_i$, it prevented

the steep fall in pH and decreased the perpetuation of acidotic pH during reperfusion. These results showing that ATPGD1 overexpression diminishes the decline in $[pH]_i$ provides direct evidence that $[pH]_i$ buffering by histidyl dipeptides may be an essential feature of the cardioprotective effects of carnosine. Nevertheless, pH buffering does not seem to be the sole mechanism of protection because perfusion with balenine, which is as efficient a buffer as carnosine, did not ameliorate I/R injury, suggesting that simply buffering $[pH]_i$ during I/R is not sufficient for limiting I/R and that properties of carnosine, other than buffering $[pH]_i$, may be pertinent to its cardioprotective effects. Nonetheless, the lack of protection by anserine, which has a lower buffering capacity than carnosine, suggests that pH buffering by carnosine is important. Because anserine has a lower buffering capacity, we suggest that both aldehyde quenching and buffering intracellular pH are important components of carnosine-mediated protection. Therefore, in comparison with previous interventions with buffers and antioxidants, carnosine has a more superior protective profile. Based on this evidence, it appears that buffering and aldehyde quenching properties of carnosine, optimized by natural selection, may be ideally suited for the protection of ischemic tissue. This property of carnosine seems to be in contrast to anserine and balenine, which are mostly abundant in avian and whale hearts,[40] suggesting that greater abundance of carnosine may be acquired by land mammals to optimize both the buffering and aldehyde-quenching properties of histidyl dipeptides.

Our findings further suggest that the mechanism linking the cardioprotective effects of carnosine may relate to the prevention of acidification and quenching of reactive aldehydes generated during I/R injury. These changes are likely to prevent metabolic derangements in ischemic tissue. Indeed, previous work has shown that interventions that promote glucose supply and use protect the heart during ischemia and improve recovery during reperfusion.[43,62–64] Clinical studies with glucose-insulin-potassium therapy, which augments glucose metabolism during acute myocardial ischemia, improves the outcome in patients receiving thrombolytic therapy.[65,66] In addition, the protective effects of buffering $[pH]_i$ may also be related to the preservation of energy metabolism. For instance, it has been reported that during ischemia, delaying $[pH]_i$ decline by proton-buffering agents preserves glycolysis and prevents myocardial injury.[67,68] Our experiments with ATPGD1 hearts provide a direct link between the two phenomena. We found that although glucose uptake in the WT and ATPGD1-Tg mice hearts was similar, lactate formation was increased, suggesting that increasing the buffering capacity during ischemia facilitates anaerobic glycolysis. That ATPGD1 hearts also showed less severe depletion of high-energy phosphates further reinforces the view that myocardial energetics could be preserved during ischemia by buffering $[pH]_i$. Whether the salutary effects of *ATPGD1* expression on glycolysis are attributed to buffering, aldehyde quenching, or direct effects on metabolic pathways requires further investigation. Nevertheless, our current data provide strong evidence that carnosine prevents oxidative stress, acidification, and metabolic derangements that are key features of myocardial I/R injury and therefore have high clinical relevance. Because carnosine is an endogenous dipeptide and its myocardial levels could be modulated by exogenous supplementation or by modulation of the endogenous production, it could be used therapeutically to promote recovery from myocardial injury or prophylactically to prevent myocardial injury in susceptible individuals.

ARTICLE INFORMATION

Received November 12, 2019; accepted March 24, 2020.

Affiliations

From the Diabetes and Obesity Center (J.Z., D.J.C., L.G., G.J., K.K., D.H., A.B., S.P.B.), Christina Lee Brown Envirome Institute (J.Z., D.J.C., L.G., G.J., K.K., D.H., A.B., S.P.B.), Division of Cardiovascular Medicine, Department of Medicine (Y.G.), Department of Chemistry (X.Z., L.H., X.Y., M.A.I.P.), University of Louisville, KY; Department of Anesthesiology and Perioperative and Pain Medicine, Stanford University, Palo Alto, CA (D.O.); Department of Medicine, The Aga Khan University, Medical College, Nairobi, Kenya (J.S.); Department of Pharmaceutical Sciences, University of Colorado, Denver, CO (A.K., V.K., M.F.W.).

Acknowledgments

We thank D. Mosley, F. Li, and the Diabetes and Obesity Center's Imaging and Physiological Core and Animal Models and Phenotyping Core at the University of Louisville for technical assistance.

Sources of Funding

This work was supported by the National Institutes of Health: R01HL122581-01 (Baba), R01HL55477, GM127607 (Bhatnagar).

Disclosures

None.

Supplementary Materials

Data S1
Table S1
Figures S1 and S2
References 21, 27, 36 and 69–79

REFERENCES

1. Hausenloy DJ, Yellon DM. Myocardial ischemia-reperfusion injury: a neglected therapeutic target. *J Clin Invest*. 2013;123:92–100.
2. Boldyrev AA, Aldini G, Derave W. Physiology and pathophysiology of carnosine. *Physiol Rev*. 2013;93:1803–1845.
3. Bate-Smith EC. The buffering of muscle in rigor: protein, phosphate and carnosine. *J Physiol (Lond)*. 1938;92:335–343.
4. Aldini G, Carini M, Beretta G, Bradamante S, Facino RM. Carnosine is a quencher of 4-hydroxy-nonenal: through what mechanism of reaction? *Biochem Biophys Res Commun*. 2002;298:699–706.
5. Carini M, Aldini G, Beretta G, Arlandini E, Facino RM. Acrolein-sequestering ability of endogenous dipeptides: characterization of carnosine and homocarnosine/acrolein adducts by electrospray ionization tandem mass spectrometry. *J Mass Spectrom*. 2003;38:996–1006.
6. Ihara H, Kakihana Y, Yamakage A, Kai K, Shibata T, Nishida M, Yamada KI, Uchida K. 2-oxo-histidine-containing dipeptides are functional oxidation products. *J Biol Chem*. 2019;294:1279–1289.

7. Bonfanti L, Peretto P, De Marchis S, Fasolo A. Carnosine-related dipeptides in the mammalian brain. *Prog Neurobiol*. 1999;59:333–353.
8. Drozak J, Veiga-da-Cunha M, Vertommen D, Stroobant V, Van Schaftingen E. Molecular identification of carnosine synthase as ATP-grasp domain-containing protein 1 (ATPGD1). *J Biol Chem*. 2010;285:9346–9356.
9. Cobbe SM, Poole-Wilson PA. The time of onset and severity of acidosis in myocardial ischaemia. *J Mol Cell Cardiol*. 1980;12:745–760.
10. Ferrari R. Metabolic disturbances during myocardial ischemia and reperfusion. *Am J Cardiol*. 1995;76:17B–24B.
11. Ferrari R, Ceconi C, Curello S, Cargnoni A, Condorelli E, Belloli S, Albertini A, Visioli O. Metabolic changes during post-ischaemic reperfusion. *J Mol Cell Cardiol*. 1988;20(suppl 2):119–133.
12. Nishida M, Borzak S, Kraemer B, Navas JP, Kelly RA, Smith TW, Marsh JD. Role of cation gradients in hypercontracture of myocytes during simulated ischemia and reperfusion. *Am J Physiol*. 1993;264:H1896–H1906.
13. Tani M, Neely JR. Role of intracellular Na+ in Ca2+ overload and depressed recovery of ventricular function of reperfused ischemic rat hearts. Possible involvement of H+-Na+ and Na+-Ca2+ exchange. *Circ Res*. 1989;65:1045–1056.
14. Avkiran M, Marber MS. Na(+)/H(+) exchange inhibitors for cardioprotective therapy: progress, problems and prospects. *J Am Coll Cardiol*. 2002;39:747–753.
15. Masereel B, Pochet L, Laeckmann D. An overview of inhibitors of Na(+)/H(+) exchanger. *Eur J Med Chem*. 2003;38:547–554.
16. Eaton P, Li JM, Hearse DJ, Shattock MJ. Formation of 4-hydroxy-2-nonenal-modified proteins in ischemic rat heart. *Am J Physiol*. 1999;276:H935–H943.
17. Dolinsky VW, Chan AY, Robillard Frayne I, Light PE, Des Rosiers C, Dyck JR. Resveratrol prevents the prohypertrophic effects of oxidative stress on LKB1. *Circulation*. 2009;119:1643–1652.
18. van der Kraaij AM, de Jonge HR, Esterbauer H, de Vente J, Steinbusch HW, Koster JF. Cumene hydroperoxide, an agent inducing lipid peroxidation, and 4-hydroxy-2,3-nonenal, a peroxidation product, cause coronary vasodilatation in perfused rat hearts by a cyclic nucleotide independent mechanism. *Cardiovasc Res*. 1990;24:144–150.
19. Ishikawa T, Esterbauer H, Sies H. Role of cardiac glutathione transferase and of the glutathione s-conjugate export system in biotransformation of 4-hydroxynonenal in the heart. *J Biol Chem*. 1986;261:1576–1581.
20. Bhatnagar A. Electrophysiological effects of 4-hydroxynonenal, an aldehydic product of lipid peroxidation, on isolated rat ventricular myocytes. *Circ Res*. 1995;76:293–304.
21. Zhao J, Posa DK, Kumar V, Hoetker D, Kumar A, Ganesan S, Riggs DW, Bhatnagar A, Wempe MF, Baba SP. Carnosine protects cardiac myocytes against lipid peroxidation products. *Amino Acids*. 2019;51:123–138.
22. Conklin DJ, Guo Y, Jagatheesan G, Kilfoil PJ, Haberzettl P, Hill BG, Baba SP, Guo L, Wetzelberger K, Obal D, et al. Genetic deficiency of glutathione s-transferase p increases myocardial sensitivity to ischemia-reperfusion injury. *Circ Res*. 2015;117:437–449.
23. Dixit BL, Balendiran GK, Watowich SJ, Srivastava S, Ramana KV, Petrash JM, Bhatnagar A, Srivastava SK. Kinetic and structural characterization of the glutathione-binding site of aldose reductase. *J Biol Chem*. 2000;275:21587–21595.
24. Srivastava S, Watowich SJ, Petrash JM, Srivastava SK, Bhatnagar A. Structural and kinetic determinants of aldehyde reduction by aldose reductase. *Biochemistry*. 1999;38:42–54.
25. Ma H, Guo R, Yu L, Zhang Y, Ren J. Aldehyde dehydrogenase 2 (ALDH2) rescues myocardial ischaemia/reperfusion injury: role of autophagy paradox and toxic aldehyde. *Eur Heart J*. 2011;32:1025–1038.
26. Shinmura K, Bolli R, Liu SQ, Tang XL, Kodani E, Xuan YT, Srivastava S, Bhatnagar A. Aldose reductase is an obligatory mediator of the late phase of ischemic preconditioning. *Circ Res*. 2002;91:240–246.
27. Baba SP, Hoetker JD, Merchant M, Klein JB, Cai J, Barski OA, Conklin DJ, Bhatnagar A. Role of aldose reductase in the metabolism and detoxification of carnosine-acrolein conjugates. *J Biol Chem*. 2013;288:28163–28179.
28. Lee JW, Miyawaki H, Bobst EV, Hester JD, Ashraf M, Bobst AM. Improved functional recovery of ischemic rat hearts due to singlet oxygen scavengers histidine and carnosine. *J Mol Cell Cardiol*. 1999;31:113–121.
29. Bae ON, Serfozo K, Baek SH, Lee KY, Dorrance A, Rumbeiha W, Fitzgerald SD, Farooq MU, Naravelta B, Bhatt A, Majid A. Safety and efficacy evaluation of carnosine, an endogenous neuroprotective agent for ischemic stroke. *Stroke*. 2013;44:205–212.
30. Teufel M, Saudek V, Ledig JP, Bernhardt A, Boularand S, Carreau A, Cairns NJ, Carter C, Cowley DJ, Duverger D, et al. Sequence identification and characterization of human carnosinase and a closely related non-specific dipeptidase. *J Biol Chem*. 2003;278:6521–6531.
31. Lombardi C, Carubelli V, Lazzarini V, Vizzardi E, Bordonali T, Ciccarese C, Castrini AI, Dei Cas A, Nodari S, Metra M. Effects of oral administration of orodispersible levo-carnosine on quality of life and exercise performance in patients with chronic heart failure. *Nutrition*. 2015;31:72–78.
32. Castro GJ, Bhatnagar A. Effect of extracellular ions and modulators of calcium transport on survival of tert-butyl hydroperoxide exposed cardiac myocytes. *Cardiovasc Res*. 1993;27:1873–1881.
33. Lee ET. *Statistical Methods for Survival Data Analysis*. Belmont, CA: Lifetime Learning Publications; 1980.
34. Peto R, Lee P. Weibull distributions for continuous-carcinogenesis experiments. *Biometrics*. 1973;29:457–470.
35. Thoman DRBL, Antle CE. Inferences on the parameters of the weibull distribution. *Technometrics*. 1969;445–460.
36. Hoetker D, Chung W, Zhang D, Zhao J, Schmidtke VK, Riggs DW, Derave W, Bhatnagar A, Bishop DJ, Baba SP. Exercise alters and beta-alanine combined with exercise augments histidyl dipeptide levels and scavenges lipid peroxidation products in human skeletal muscle. *J Appl Physiol*. 2018;125:1767–1778.
37. Hill CA, Harris RC, Kim HJ, Harris BD, Sale C, Boobis LH, Kim CK, Wise JA. Influence of beta-alanine supplementation on skeletal muscle carnosine concentrations and high intensity cycling capacity. *Amino Acids*. 2007;32:225–233.
38. Drozak J, Chrobok L, Poleszak O, Jagielski AK, Derlacz R. Molecular identification of carnosine n-methyltransferase as chicken histamine n-methyltransferase-like protein (HNMT-like). *PLoS ONE*. 2013;8:e64805.
39. Barski OA, Xie Z, Baba SP, Sithu SD, Agarwal A, Cai J, Bhatnagar A, Srivastava S. Dietary carnosine prevents early atherosclerotic lesion formation in apolipoprotein e-null mice. *Arterioscler Thromb Vasc Biol*. 2013;33:1162–1170.
40. Abe H. Role of histidine-related compounds as intracellular proton buffering constituents in vertebrate muscle. *Biochemistry (Mosc)*. 2000;65:757–765.
41. Maroko PR, Libby P, Sobel BE, Bloor CM, Sybers HD, Shell WE, Covell JW, Braunwald E. Effect of glucose-insulin-potassium infusion on myocardial infarction following experimental coronary artery occlusion. *Circulation*. 1972;45:1160–1175.
42. Opie LH, Owen P. Effect of glucose-insulin-potassium infusions on arteriovenous differences of glucose of free fatty acids and on tissue metabolic changes in dogs with developing myocardial infarction. *Am J Cardiol*. 1976;38:310–321.
43. Stanley WC, Lopaschuk GD, Hall JL, McCormack JG. Regulation of myocardial carbohydrate metabolism under normal and ischaemic conditions. Potential for pharmacological interventions. *Cardiovasc Res*. 1997;33:243–257.
44. Trexler ET, Smith-Ryan AE, Stout JR, Hoffman JR, Wilborn CD, Sale C, Kreider RB, Jager R, Earnest CP, Bannock L, et al. International Society of Sports Nutrition position stand: beta-alanine. *J Int Soc Sports Nutr*. 2015;12:30.
45. Harris RC, Tallon MJ, Dunnett M, Boobis L, Coakley J, Kim HJ, Fallowfield JL, Hill CA, Sale C, Wise JA. The absorption of orally supplied beta-alanine and its effect on muscle carnosine synthesis in human vastus lateralis. *Amino Acids*. 2006;30:279–289.
46. Ansurudeen I, Sunkari VG, Grunler J, Peters V, Schmitt CP, Catrina SB, Brismar K, Forsberg EA. Carnosine enhances diabetic wound healing in the *db/db* mouse model of type 2 diabetes. *Amino Acids*. 2012;43:127–134.
47. Lee JW, Bobst EV, Wang YG, Ashraf MM, Bobst AM. Increased endogenous ascorbyl free radical formation with singlet oxygen scavengers in reperfusion injury: an EPR and functional recovery study in rat hearts. *Cell Mol Biol (Noisy-le-grand)*. 2000;46:1383–1395.
48. Esterbauer H, Schaur RJ, Zollner H. Chemistry and biochemistry of 4-hydroxynonenal, malonaldehyde and related aldehydes. *Free Radic Biol Med*. 1991;11:81–128.
49. Awashti YC. *Toxicology of Glutathione Transferases*. Galveston, TX: Taylor & Francis; 2007.
50. Blasig IE, Grune T, Schonheit K, Rohde E, Jakstadt M, Haseloff RF, Siems WG. 4-hydroxynonenal, a novel indicator of lipid peroxidation for reperfusion injury of the myocardium. *Am J Physiol*. 1995;269:H14–H22.

51. Takabe W, Niki E, Uchida K, Yamada S, Satoh K, Noguchi N. Oxidative stress promotes the development of transformation: involvement of a potent mutagenic lipid peroxidation product, acrolein. *Carcinogenesis*. 2001;22:935–941.
52. Uchida K, Stadtman ER. Covalent attachment of 4-hydroxynonenal to glyceraldehyde-3-phosphate dehydrogenase. A possible involvement of intra- and intermolecular cross-linking reaction. *J Biol Chem*. 1993;268:6388–6393.
53. Uchida K, Szweda LI, Chae HZ, Stadtman ER. Immunochemical detection of 4-hydroxynonenal protein adducts in oxidized hepatocytes. *Proc Natl Acad Sci USA*. 1993;90:8742–8746.
54. Harris RC, Marlin DJ, Dunnett M, Snow DH, Hultman E. Muscle buffering capacity and dipeptide content in the thoroughbred horse, greyhound dog and man. *Comp Biochem Physiol A Comp Physiol*. 1990;97:249–251.
55. Parkhouse WS, McKenzie DC, Hochachka PW, Ovalle WK. Buffering capacity of deproteinized human vastus lateralis muscle. *J Appl Physiol*. 1985;58:14–17.
56. Wisloff U, Loennechen JP, Falck G, Beisvag V, Currie S, Smith G, Ellingsen O. Increased contractility and calcium sensitivity in cardiac myocytes isolated from endurance trained rats. *Cardiovasc Res*. 2001;50:495–508.
57. Danes VR, Anthony J, Rayani K, Spitzer KW, Tibbits GF. Ph recovery from a proton load in rat cardiomyocytes: effects of chronic exercise. *Am J Physiol Heart Circ Physiol*. 2018;314:H285–H292.
58. Opie LH, Mansford KR, Owen P. Effects of increased heart work on glycolysis and adenine nucleotides in the perfused heart of normal and diabetic rats. *Biochem J*. 1971;124:475–490.
59. Schaffer SW, Safer B, Ford C, Illingworth J, Williamson JR. Respiratory acidosis and its reversibility in perfused rat heart: regulation of citric acid cycle activity. *Am J Physiol*. 1978;234:H40–H51.
60. Cingolani HE, Mattiazzi AR, Blesa ES, Gonzalez NC. Contractility in isolated mammalian heart muscle after acid-base changes. *Circ Res*. 1970;26:269–278.
61. Swietach P, Youm JB, Saegusa N, Leem CH, Spitzer KW, Vaughan-Jones RD. Coupled Ca2+/H+ transport by cytoplasmic buffers regulates local Ca2+ and H+ ion signaling. *Proc Natl Acad Sci USA*. 2013;110:E2064–E2073.
62. Hwang YC, Bakr S, Ramasamy R, Bergmann SR. Relative importance of enhanced glucose uptake versus attenuation of long-chain acyl carnitines in protecting ischemic myocardium. *Coron Artery Dis*. 2002;13:313–318.
63. Stanley WC, Chandler MP. Energy metabolism in the normal and failing heart: potential for therapeutic interventions. *Heart Fail Rev*. 2002;7:115–130.
64. Ramasamy R, Trueblood N, Schaefer S. Metabolic effects of aldose reductase inhibition during low-flow ischemia and reperfusion. *Am J Physiol*. 1998;275:H195–H203.
65. Fath-Ordoubadi F, Beatt KJ. Glucose-insulin-potassium therapy for treatment of acute myocardial infarction: an overview of randomized placebo-controlled trials. *Circulation*. 1997;96:1152–1156.
66. Diaz R, Paolasso EA, Piegas LS, Tajer CD, Moreno MG, Corvalan R, Isea JE, Romero G. Metabolic modulation of acute myocardial infarction. The ECLA (Estudios Cardiologicos Latino America) collaborative group. *Circulation*. 1998;98:2227–2234.
67. Takeuchi K, Buenaventura P, Cao-Danh H, Glynn P, Simplaceanu E, McGowan FX, del Nido PJ. Improved protection of the hypertrophied left ventricle by histidine-containing cardioplegia. *Circulation*. 1995;92:395–399.
68. McGowan FX Jr, Cao-Danh H, Takeuchi K, Davis PJ, del Nido PJ. Prolonged neonatal myocardial preservation with a highly buffered low-calcium solution. *J Thorac Cardiovasc Surg*. 1994;108:772–779.
69. Guo Y, Wu WJ, Qiu Y, Tang XL, Yang Z, Bolli R. Demonstration of an early and a late phase of ischemic preconditioning in mice. *Am J Physiol*. 1998;275:H1375–H1387.
70. Guo Y, Jones WK, Xuan YT, Tang XL, Bao W, Wu WJ, Han H, Laubach VE, Ping P, Yang Z, et al. The late phase of ischemic preconditioning is abrogated by targeted disruption of the inducible no synthase gene. *Proc Natl Acad Sci USA*. 1999;96:11507–11512.
71. Flaherty MP, Guo Y, Tiwari S, Rezazadeh A, Hunt G, Sanganalmath SK, Tang XL, Bolli R, Dawn B. The role of TNF-alpha receptors p55 and p75 in acute myocardial ischemia/reperfusion injury and late preconditioning. *J Mol Cell Cardiol*. 2008;45:735–741.
72. He H, Javadpour MM, Latif F, Tardiff JC, Ingwall JS. R-92I and R-92W mutations in cardiac troponin T lead to distinct energetic phenotypes in intact mouse hearts. *Biophys J*. 2007;93:1834–1844.
73. Bretthorst GL, Kotyk JJ, Ackerman JJ. 31P NMR Bayesian spectral analysis of rat brain in vivo. *Magn Reson Med*. 1989;9:282–287.
74. Keith RJ, Haberzettl P, Vladykovskaya E, Hill BG, Kaiserova K, Srivastava S, Barski O, Bhatnagar A. Aldose reductase decreases endoplasmic reticulum stress in ischemic hearts. *Chem Biol Interact*. 2009;178:242–249.
75. Klavins K, Drexler H, Hann S, Koellensperger G. Quantitative metabolite profiling utilizing parallel column analysis for simultaneous reversed-phase and hydrophilic interaction liquid chromatography separations combined with tandem mass spectrometry. *Anal Chem*. 2014;86:4145–4150.
76. Wei X, Sun W, Shi X, Koo I, Wang B, Zhang J, Yin X, Tang Y, Bogdanov B, Kim S, et al. Metsign: a computational platform for high-resolution mass spectrometry-based metabolomics. *Anal Chem*. 2011;83:7668–7675.
77. Wei X, Shi X, Kim S, Patrick JS, Binkley J, Kong M, McClain C, Zhang X. Data dependent chromatographic peak model-based spectrum deconvolution for analysis of LC-MS data. *Anal Chem*. 2014;86:2156–2165.
78. Wei X, Shi X, Kim S, Zhang L, Patrick JS, Binkley J, McClain C, Zhang X. Data preprocessing method for liquid chromatography-mass spectrometry based metabolomics. *Anal Chem*. 2012;84:7963–7971.
79. Baba SP, Zhang D, Singh M, Dassanayaka S, Xie Z, Jagatheesan G, Zhao J, Schmidtke VK, Brittian KR, Merchant ML, et al. Deficiency of aldose reductase exacerbates early pressure overload-induced cardiac dysfunction and autophagy in mice. *J Mol Cell Cardiol*. 2018;118:183–192.

SUPPLEMENTAL MATERIAL

Data S1.

SUPPLEMENTAL MATERIALS AND METHODS

Enhance histidyl dipeptide levels within the cardiac tissue

***β-Alanine and carnosine feeding*.** To enhance histidyl dipeptide pool within cardiac tissue, we treated WT C57BL/6 mice (12-14 week) with β-alanine (20 g/L) or carnosine (10 g/L) in drinking water or water alone for seven days. Heart and skeletal muscle from the treated and untreated mice were collected and analyzed for different histidyl dipeptides levels using LC/MS.

Generation of cardio specific carnosine synthase (ATPGD1) transgenic mice*.* To enhance endogenous production of histidyl dipeptides within cardiac tissue, we generated cardio specific ATPGD1 transgenic (Tg) mice. Full protein-coding sequence of the mouse (m) ATPGD1 cDNA (2.84 kb a kind gift from Dr. Emile Van Schaftingen, Ludwig Institute for Cancer Research, Universite Catholique de Louvain, Belgium) was cloned under the control of mouse alpha-myosin heavy chain promoter (α-MHC; 5.5 kb), 0.6 Kb HGH (human growth hormone) poly A was ligated at the 3' end of the minigene construct. Nucleotide sequencing and comparisons with published sequences verified the construct as m*ATPGD*1 cDNA. The resultant transgene (9.04 Kb) composed of α-MHC promoter, the entire protein-coding region of ATPGD1 and HGH polyadenylation signal sequence. The transgene construct was linearized, purified, and microinjected into the pronuclei of fertilized ova to generate α-*MHC*-ATPGD1-Tg mice at the University of Cincinnati, Cincinnati, OH Transgenic Core. Four transgenic founders with the varying copy number of the transgene were generated on the C57Bl/6 background. Founder mice were identified by genomic PCR using the following primers: Forward-5'- *AGT CCT GGT GGG AGA GCC ATA* -3' and Reverse 5' – *GCC AAG CAG GGG ACA GGC AAA* -3' corresponding to *α-MHC* 5'UTR and the *ATPGD1* coding region, respectively. Two transgenic (TG) lines were established and distinguished from their non-transgenic wild type littermates (WT) cohorts by PCR.

Myocardial ischemia and reperfusion (I/R) injury in-vivo and assessment of area at risk and infarct size.

The I/R injury was produced by subjecting mice to a 30 min of coronary occlusion followed by 24 h of reperfusion as described previously[69-71]. Briefly, the mice (10-14 weeks of age) were anesthetized with pentobarbital sodium (50mg/kg, i.p) intubated and ventilated at room air supplemented with oxygen. The body temperature was monitored with a rectal probe and maintained at 37±0.2°C with a heating pad. To replace blood loss, blood from a donor mouse was given intravenously. The chest was opened through a midline sternotomy, and a nontraumatic balloon occluder was applied on the left anterior descending coronary artery 2-3 mm from the tip of left auricle. Successful performance of the surgery was verified by noting the development of a pale color in the distal myocardium on inflation of the balloon and return of a bright red color due to hyperemia after deflation and by observing the ST-segment elevation and widening of the QRS complex on the ECG during ischemia and their resolution after reperfusion. Following the coronary occlusion/reperfusion, the chest was closed in layers, and the mice were allowed to recover under close monitoring. Heart was excised and perfused with Krebs-Henseleit (KH) solution through an aortic cannula. To determine the area of infarcted myocardium from the viable myocardium, the heart was perfused with 1% triphenyl tetrazolium chloride in phosphate buffer. To delineate the area of occlusion, the coronary artery was tied at the site of previous occlusion, and the aortic root was perfused with 10% Pthalo blue dye. The region of risk was identified by the absence of blue dye, whereas the rest of left ventricle was stained dark blue. The left ventricle was cut into transverse slices, which were fixed in 10% neutral buffered formaldehyde, weighed, and photographed under a microscope. The corresponding areas were measured by computerized planimetry and from these measurements; the infarct size was calculated as the percentage of region at risk.

In the second set of experiments, coronary ligation was performed, to analyze the formation of aldehyde protein adduct during ischemic injury. Hearts from the WT and ATPGD1-Tg mice were collected following 40 min of ligation. The ischemic zone of ligated mice and the anterior zone of sham-operated mice were clamp frozen and analyzed by Western blotting.

Langendorff perfusion

***Global ischemia-reperfusion (I/R) ex vivo*.** To exclude the neurohormonal effects associated with *in-vivo* model of I/R, we performed I/R in a Langendorff mode as described previously[27]. Mice were anesthetized (sodium pentobarbital, 60mg/kg body weight, heparin, 10 units/g body weight), the thorax of mice was opened and the hearts were removed, placed immediately in the ice-cold KH buffer; mM 118 NaCl, 4.7 KCl, $MgCl_2$, $CaCl_2$, KH_2PO_4, $NaHCO_3$ and 11 glucose. The buffer was heated at 37°C and continuously gassed (95% O_2, 5%CO_2). Hearts from the WT and ATPGD1-Tg, mice were continuously perfused at a constant pressure of 80 mmHg in the Langendorff mode and after 20-30 min of perfusion, the isolated hearts were subjected to 30 min of ischemia followed by 45 min of reperfusion. Functional recovery of the hearts was measured by placing a food grade plastic wrap, fluid-filled balloon to a pressure of 5-8 mm Hg. Left ventricular pressure was recorded using an APT300 pressure transducer (Harvard Apparatus, Holliston, MA) connected to a ML221 bridge amplifier, a Power lab 16/30 A/D board, and a PC running Lab Chart Pro v7 (AD Instruments, Colorado Springs, CO). Perfusion flow rate was monitored using a 1PXN inline probe and TS410 flowmeter (transonic Systems Inc., Ithaca, NY) and was typically between 1.5 and 2 mL/min. Left ventricular developed pressure was derived from the pressure trace as the difference between systolic and diastolic pressures. Perfusates were collected on ice and the levels of creatinine kinase (CK) and lactate dehydrogenase (LDH) were measured using kits purchased from Thermo-Electron.

In a second line of experiments, we tested which dipeptide analogue could lead to recovery of function following ischemia. For these experiments, wild type (WT) C57/Bl6 mice (12-14 weeks old) were perfused with either balenine and anserine (1mM), followed by 30 min of ischemia and 45 min of reperfusion and the recovery of cardiac function was monitored in a Langendorff mode as described above.

Low flow ischemia and ^{13}C D-glucose perfusion: To determine whether ATPGD1 *o*verexpression influences the glycolytic fluxes during ischemic injury, isolated WT and ATPGD1-Tg mice hearts were perfused in the Langendorff mode for 10 min in a KH buffer; mM 118 NaCl, 4.7 KCl, $MgCl_2$, $CaCl_2$, KH_2PO_4, $NaHCO_3$ and 11 ^{13}C-D-glucose followed by 15 min of low flow ischemia (LFI, 10% of baseline). The effluent was collected at regular intervals and analyzed for ^{13}C D-glucose and ^{13}C lactate.

^{31}P Nuclear Magnetic Resonance Spectroscopy*:* Hearts isolated from the WT and ATPGD1-Tg mice were perfused in a Langendorff mode with KH buffer at constant coronary pressure of 75 mmHg at 37°C for 10 min followed by 20 min LFI (10% of baseline) and 50 min reperfusion. ^{31}P-NMR spectra were collected continuously and simultaneously during measurement of isovolumic contractile performance using ^{31}P-NMR spectroscopy. [72] Isolated perfused hearts and an external standard containing 4.51 μmol of phenylphosphonic acid (PPA) in a small sealed plastic tube were placed in a 10-mm glass NMR sample tube and inserted into a 10 mm Varian broad band probe situated in an 89-mm bore 9.4-T superconducting magnet. To improve homogeneity of the NMR-sensitive volume, the perfusate level was adjusted so that the heart was submerged in buffer. ^{31}P-NMR spectra were obtained using 60° pulses and a recycle time of 2.4 S, 6,000-Hz sweep width and 2 K data points at 161.94 MHz using a Varian Inova spectrometer (Varian Inc., Palo Alto, CA). Single spectra were collected during 10 min periods and consisted of data averaged from 256 free induction decays. Spectra were processed using 20-Hz exponential multiplication and zero and first-order phase corrections. The resonance areas of phosphocreatine (PCr), ATP, inorganic phosphate (Pi) and the chemical shifts of Pi were quantified using Bayesian Analysis Software (G.L. Bretthorst Washington University, St. Louis, MO) [73]. By comparing the amplitude under the peaks from fully relaxed (recycle time 15 sec) and those of partially saturated (recycle time 2.4 sec) spectra, the correction factors for saturation were calculated for ATP (1.041), PCr (1.285), Pi (1.157) and PPA (1.283).

Cell culture studies

Isolation of adult cardiomyocytes*.* Cardiac myocytes from the WT and ATPGD1-Tg mice hearts (age 12-16 weeks) were isolated using Langendorff perfusion as described previously.[74] [21] Isolated hearts from these mice were rinsed in physiological saline and perfused with oxygenated (95% O_2- 5%CO_2), Ca^{2+}- free modified Tyrode bicarbonate buffer (buffer A mM: NaCl 126, KCL 4.4, $MgCl_2$ 1.0, $NaHCO_3$ 18, glucose 11, HEPES 4, 2,3 butanedione monoxime 10, taurine 30, pH 7.35) at 37°C for 5 min. The extracellular matrix was digested by buffer containing buffer A with Liberase Blendzyme type I 0.25 mg/mL, 1mg/mL albumin, 0.015 mg/mL DNase, 0.015 mg/mL proteinase in the 50 mL of recirculating digestion buffer (buffer A with 25 μM $CaCl_2$) for 12-15

min. Hearts were separated in mincing buffer (10 mL digestion buffer with 9 mg/mL albumin and Liberase) and cells were allowed to settle. $CaCl_2$ was reintroduced in a graded fashion at 5- min intervals (five total steps) to sequentially increase the Ca^{2+} concentration to 500 μM.

Hypoxia reoxygenation of adult cardiomyocytes*.* Cardiomyocytes isolated from WT and ATPGD1-TG mice hearts were subjected to 2-3 h of hypoxia using a controlled hypoxic chamber (Billups-Rothenberg Modulao, Incubator Chamber) maintained at 37°C. Freshly isolated cells were maintained in serum free/ glucose free HEPES-buffered medium (mM: NaCl 113, KCL 4.7, HEPES 10, $MgSO_4$ 1.2, taurine 30, $CaCl_2$ 1, pH 6.2) at 37°C. Cells were allowed to settle down, supernatant was removed and replaced with hypoxia buffer (glucose free/serum free HEPES buffered medium that was bubbled with nitrogen (N_2). The dishes were filled with 1 mL of hypoxia buffer and incubated in a humidified hypoxic chamber containing: 1% O_2, 5% CO_2 and 94% N_2 at 37°C. Following hypoxia, the cells were re oxygenated with 1 mL of HEPES buffered medium supplemented with serum (10%) and glucose (11 mM) bubbled with O_2 and placed under normoxic conditions. For control conditions, freshly isolated cells were washed twice with a HEPES-buffered medium supplemented with serum (5%) and glucose (5.5 mM) and placed under normoxic conditions. Reoxygenation was mimicked by adding 1 mL of the medium. The supernatant was collected and analyzed for LDH release.

Superfusion of isolated cardiomyocytes with HNE and acrolein. To examine whether the increase in endogenous production of histidyl dipeptides protects against aldehyde induced hypercontracture, adult cardiomyocytes from the WT and ATPGD1-Tg mice hearts were superfused with 50-60 μM HNE or 5 μM acrolein for 60 min as described previously.[21] Digital images of approx. 100 cardiomyocyte/field were acquired at 5 min interval to quantify the number of hypercontracted and non-hypercontracted cells following aldehyde treatment.

Western blot analysis

The anterior zone of sham operated and ischemic zone of the ligated mice hearts were homogenized and separated by SDS-PAGE. Tissues were homogenized in RIPA buffer (20mM Tris-HCl pH7.5, 150 mM NaCl, 1mM EDTA, 1mM EDTA, 1mMEGTA, 1% NP-40) and separated by SDS-PAGE. Immunoblots were developed

using anti-acrolein (0.25 μg/ mL, Novus Biological), anti-HNE (0.5 μg/mL, Abcam) and anti- ATPGD1 (0.25 μg/ mL COSMO Bio Company) antibodies. Western blots were developed using ECL Plus reagent and detected with a Typhoon 9400 Variable mode imager. Band intensity was quantified by using an Image Quant TL software and bands were normalized to amido black or tubulin.

LC/MS studies

Measurement of histidyl dipeptides by LC/MS. Histidyl dipeptides in the heart and skeletal muscle were measured by LC/MS as described previously[36]. Briefly the isolated tissues from mice were homogenized in extraction buffer containing 10 mM HCl and 200 μM tyrosine-histidine as an internal standard (IS). Homogenates were sonicated on ice for 10 s, centrifuged at 16,000 × g for 10 min at 4°C. Supernatants were injected into TQ-S micro mass spectrometer in positive mode, the samples were diluted in 75% acetonitrile/25% water. The dipeptides were separated and identified by using Water ACQUITY UPLV H-Class system coupled with a Xevo TQ-S micro triple quadrupole mass spectrometer (MS). The analytes were separated by a Waters Acquity BEH HILIC column (1.7μm, 2.1× 50) equipped with an in-line frit filter unit. The analytes were eluted by using a binary solvent system consisting of 10 mM ammonium formate, 0.125% formic acid in 50% acetonitrile/50% water for mobile phase A and 10 mM ammonium formate 0.125% formic acid in 95% acetonitrile/5% water for mobile phase B at a flow rated of 0.55 ml/min. Initial conditions were 0.1:99.9 A/B ramping to 99.9:0.1 A/B over 5 min then quickly ramping to 0.1:99.9 A/B over 0.5 min. This initial composition was held from 5.5 to 8 min to equilibrate the column for the next injection. Dipeptides were quantified using the LC/MS calibration curve of relative area of carnosine and anserine to internal standard tyrosine-histidine and expressed as mole/mg wet wt. or mole/mg protein. For carnosine *m/z* 227→110, anserine *m/z* 241→110, and tyrosine-histidine m/*z* 319→110, Da MRM transitions were followed.

^{13}C glucose and ^{13}C lactate analysis.

Perfusates collected from the WT and ATPGD1-Tg hearts perfused with ^{13}C glucose and subjected to low flow ischemia as described above were dried and dissolved in 200 μL 20% acetonitrile and vigorously vortex-

mixed for 3 min. After centrifugation at 14,000 rpm, 4 ^{o}C for 20 min, the supernatant was collected for 2DLC-MS/MS analysis.

All samples were analyzed on a Thermo Q Exactive HF Hybrid Quadrupole-Orbitrap Mass Spectrometer coupled with a Thermo DIONEX UltiMate 3000 HPLC system (Thermo Fisher Scientific, Waltham, MA, USA). The UltiMate 3000 HPLC system was equipped with a reverse phase chromatography (RPC) column and a hydrophilic interaction chromatography (HILIC) column. The RPC column was an ACQUITY UPLC HSS T3 column (150 × 2.1 mm i.d., 1.8 µm) purchased from Waters (Milford, MA, USA). The HILIC column was a SeQuant® ZIC®-cHILIC HPLC column (150 × 2.1 mm i.d., 3 µm) purchased from Phenomenex (Torrance, CA, USA). The two columns were configured in parallel 2DLC mode [75]. For 2DLC separation, H_2O with 0.1% formic acid was used as the mobile phase A for RPC and 10 mM ammonium acetate (pH 3.25) was used as the mobile phase A for HILIC. Acetonitrile with 0.1% formic acid was used as mobile phase B for both RPC and HILIC. The RPC gradient was as follows: 0 min, 5% B, hold for 5.0 min; 5.0 min to 6.1 min, 5% B to 15% B; 6.1 min to 10.0 min, 15% B to 60% B, hold for 2.0 min; 12.0 min to 14.0 min, 60% B to 100% B, hold for 13.0 min; 27.0 min to 27.1 min, 100% B to 5% B, hold for 12.9 min. The gradient for HILIC separation was: 0 to 5.0 min, 95% B to 35% B, hold for 1.0 min; 6.0 min to 6.1 min, 35% B to 5% B, hold for 16.9 min; 23.0 min to 23.1 min, 5% B to 95% B, hold for 16.9 min. The flow rate was 0.4 mL/min for RPC and 0.3 mL/min for HILIC. The column temperature was 40 °C for both columns. The injection volume was 2 µL for each column.

To avoid systemic bias, the samples were analyzed by 2DLC-MS in a random order. All samples were first analyzed by 2DLC-MS positive mode followed by 2DLC-MS negative mode, to obtain the full MS data of each metabolite. For quality control purpose, a group-based pooled sample was prepared by mixing a small portion of the supernatant from all unlabeled samples in one group. One pooled sample was analyzed by 2DLC-MS after injection of every 5 biological samples. All pooled samples were analyzed by 2DLC-MS/MS in positive and negative mode respectively to acquire MS/MS spectra of each metabolite at three collision energies (20 eV, 40 eV and 60 eV).

MetSign software was used for spectrum deconvolution, metabolite identification, cross-sample peak list alignment, normalization, and statistical analysis [76-78]. To identify metabolites, the 2DLC-MS/MS data of the

pooled samples were first matched to an in-house MS/MS database that contains the parent ion m/z, MS/MS spectra, and retention time of 205 metabolite standards. The thresholds used for metabolite identification were MS/MS spectral similarity ≥ 0.4, retention time difference ≤ 0.15 min, and m/z difference ≤ 4 ppm. The 2DLC-MS/MS data without a match in the in-house database were then analyzed using Compound Discoverer software (v2.0, Thermo Fisher Scientific, Inc., Germany), where the threshold of MS/MS spectrum similarity score was set as ≥ 40 with a maximum score of 100. The remaining peaks that did not have a match were then matched to the metabolites in -house MS/MS database using the parent ion m/z and retention time to identify metabolites that do not have MS/MS spectra. The thresholds for assignment were parent ion m/z ≤ 4 ppm and retention time difference ≤ 0.15 min.

Synthesis of histidyl dipeptide analogues anserine and balenine

(a) Balenine was synthesized as mentioned previously.[21]

(b) Anserine synthesis

(S)-Methyl 3-(1H-imidazol-5-yl)-2-(2,2,2-trifluoroacetamido) propanoate (3):

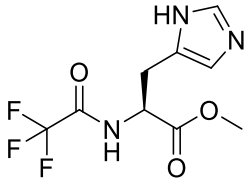

3

To L-histidine dihydrochloride (5.00 g, 20.65 mmol) in methanol (100 mL), we added ethyl 2,2,2-trifluoroacetate (2.70 mL, 22.72 mmol) and triethyl amine (1.52 mL, 82.6 mmol) and the reaction mixture was stirred for 5 h at room temperature (RT). The solvent was evaporated to dryness and the obtained solid was purified by silica gel chromatography to get the desired product, (*S*)-methyl 3-(1*H*-imidazol-5-yl)-2-(2,2,2-trifluoroacetamido) propanoate, (**3**, 4.10 g, 75% yield) as an off-white solid compound.

^{1}H NMR (D_2O, 400 MHz): δ 7.60 (s, 1H), 6.87 (s, 1H), 4.76 – 4.67 (m, 1H), 3.66 (s, 3H), 3.17 – 2.96 (m, 2H) ppm.

(S)-Methyl 2-(2,2,2-trifluoroacetamido)-3-(1-trityl-1H-imidazol-4-yl) propanoate (4):

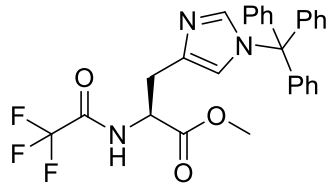

4

Trityl chloride (5.60 g, 20.36 mmol) and triethyl amine (8.53 mL, 61.53 mmol) were dissolved in anhydrous benzene (100mL) and (*S*)-methyl3-(1*H*-imidazol-5-yl)-2-(2,2,2-trifluoroacetamido) propanoate (**3**, 5.40 g, 20.36 mmol) was added. The resulting reaction mixture was refluxed for 1 h and the solvent was evaporated. Obtained semi pure compound was purified with silica gel column using dichloromethane and methanol was used as eluents to get (*S*)-methyl 2-(2,2,2-trifluoroacetamido)-3-(1-trityl-1*H*-imidazol-4-yl) propanoate (**4**, 5.80 g, 55% yield) as an off-white solid compound.

^{1}H NMR ($CDCl_3$, 400 MHz): δ 8.89 – 8.87 (d, 1H), 7.40 (s, 1H), 7.37 – 7.30 (m, 9H), 7.13 – 7.07 (m, 6H), 6.57 (s, 1H), 4.85 – 4.79 (m, 1H), 3.63 (s, 3H), 3.16 – 3.11 (m, 1H), 3.06 – 3.00 (m, 1H) ppm.

(S)-4-(3-Methoxy-3-oxo-2-(2,2,2-trifluoroacetamido) propyl)-3-methyl-1-trityl-1H-imidazol-3-ium iodide (5):

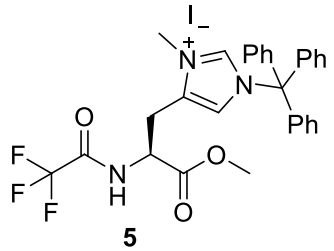

5

(*S*)-Methyl 2-(2,2,2-trifluoroacetamido)-3-(1-trityl-1*H*-imidazol-4-yl) propanoate (3.50 g, 6.90 mmol) was dissolved in anhydrous acetonitrile (100 mL) and methyl iodide (0.86 mL, 13.80 mmol) was added. The resulting reaction mixture was refluxed for 1 h and the solvent was evaporated. Obtained crude was purified with silica gel column using dichloromethane and methanol as eluents to get (*S*)-4-(3-methoxy-3-oxo-2-(2,2,2-trifluoroacetamido) propyl)-3-methyl-1-trityl-1*H*-imidazol-3-ium iodide (**5**, 4.0 g, 89% yield) as a yellow solid compound.

^{1}H NMR ($CDCl_3$, 400 MHz): δ 8.26 – 8.25 (d, 1H), 7.48 – 7.38 (m, 7H), 7.35 – 7.20 (m, 10H), 4.86 - 4.79 (m, 1H), 4.03 (s, 3H), 3.78 (s, 3H), 3.56 – 3.41 (m, 2H) ppm.

(S)-1-Carboxy-2-(1-methyl-1H-imidazol-5-yl)ethanaminium chloride (6):

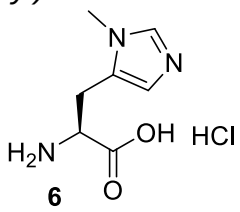

6

In a round bottom flask, we added (*S*)-4-(3-methoxy-3-oxo-2-(2,2,2-trifluoroacetamido) propyl)-3-methyl-1-trityl-1*H*-imidazol-3-ium iodide (**5**, 4.0 g, 6.16 mmol) and 4N HCl (100 mL). The reaction mixture was refluxed for 6 h, and evaporated to dryness, and the solid obtained was washed with hexanes and dried to get (*S*)-1-carboxy-2-(1-methyl-1*H*-imidazol-5-yl) ethanaminium chloride, (**6**, 1.10 g, 87% yield) as a yellow solid compound.

^{1}H NMR (D_2O, 400 MHz): δ 8.62 (s, 1H), 7.36 (s, 1H), 4.26 – 4.19 (m, 1H), 3.78 (s, 3H), 3.41 – 3.25 (m, 2H) ppm.

(S)-Methyl 2-amino-3-(1-methyl-1H-imidazol-4-yl) propanoate hydrochloride (7):

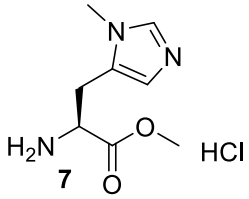

7

In 300 mL of methanolic hydrochloric acid was added (*S*)-2-amino-3-(1-methyl-1*H*-imidazol-5-yl) propanoic acid hydrochloride (2.60 g, 12.64 mmol) at room temperature. The reaction mixture was then refluxed for 48 h, and evaporated to dryness to get (*S*)-methyl 2-amino-3-(1-methyl-1*H*-imidazol-4-yl) propanoate hydrochloride, (**7**, 2.5 g, 90% yield) as a white solid. (Note: Methanolic-HCl was made by purging HCl gas into required methanol for 5 min.)

^{1}H NMR (D_2O, 400 MHz): δ 8.62 (s, 1H), 7.39 (s, 1H), 4.45 – 4.19 (m, 1H), 3.78 (s, 3H), 3.76 (s, 3H), 3.47 - 3.26 (m, 2H) ppm.

(*S*)-Methyl 2-(3-(*tert*-butoxycarbonylamino) propanamido)-3-(1-methyl-1H-imidazol-5-yl) propanoate (8):

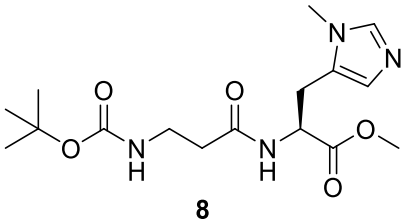

8

Added sequentially to a reaction flask under nitrogen were (*S*)-methyl 2-amino-3-(1-methyl-1*H*-imidazol-5-yl)propanoate hydrochloride (**7**, 2.0 g, 9.10 mmol), boc-b-alanine (1.89 g, 10.02 mmol), EDC (N-(3-Dimethylaminopropyl)-N′-ethylcarbodiimide) (1.92 g, 10.02 mmol) followed by DCM (100 mL) and then *N*-methylmorpholine (4.00 mL, 36.4 mmol via syringe). The contents were stirred at room temperature under nitrogen and the solids gradually dissolved. The contents were stirred at room temperature for 24 h, and then slowly diluted into iced water and extracted with DCM. The organic phase was dried evaporated and chromatographed using dichloromethane and methanol as eluents to get (*S*)-methyl 2-(3-(*tert*-butoxycarbonylamino) propanamido)-3-(1-methyl-1*H*-imidazol-5-yl) propanoate (**8**, 2.0 g, 62% yield) as an off-white solid compound.

^{1}H NMR ($CDCl_3$, 400 MHz): δ 7.37 (s, 1H), 6.75 (s, 1H), 6.66 – 6.50 (m, 1H), 5.15 – 5.08 (m, 1H), 4.82 – 4.77 (m, 1H), 3.74 (s, 3H), 3.57 (s, 3H), 3.45 – 3.30 (m, 3H), 3.16 – 3.02 (m, 1H), 2.50 – 2.35 (m, 2H), 1.42 (s, 9H) ppm.

L-Anserine (9):

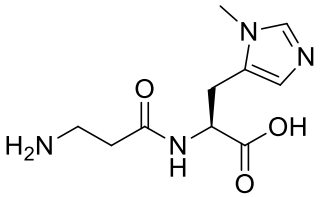

L-Anserine

To (*S*)-methyl 2-(3-(tert-butoxycarbonylamino) propanamido)-3-(1-methyl-1*H*-imidazol-4-yl) propanoate (**8,** 2.2 g, 6.2 mmol) was added 2N NaOH (18.6 mL) in THF (50 mL) and methanol (50 mL) and the reaction was stirred for the 24 h at RT. Solvent was evaporated and the reaction mixture

was neutralized by 1N HCl to pH 3. It was further stirred and neutralized by aqueous saturated sodium bicarbonate solution. All the water was evaporated to dryness and the obtained solid was triturated with DCM and dried again. The obtained solid was dissolved in hot ethanol and passed through the celite plug, twice. Filtrate was evaporated and dried under high vacuum to get the L-anserine (**9**, 1.30 g, 87% yield) as a white solid compound.

^{1}H NMR (D_2O, 400 MHz): δ 8.61 (s, 1H), 7.27 (s, 1H), 4.54 – 4.50 (m, 1H), 3.86 (s, 3H), 3.31 – 3.19 (m, 3H), 3.14 – 3.07 (m, 1H), 2.80 – 2.64 (m, 2H) ppm; ^{13}C NMR (D_2O, 100 MHz) *δ* 176.3, 171.7, 135.1, 131.3, 117.5, 53.2, 35.2, 33.1, 31.9, 25.8.

Echocardiographic analysis of cardiac function

Transthoracic echocardiography of the left ventricle was performed using a Vevo 770 echocardiography system as described previously. [79] Briefly the body temperature of the mice was maintained (36.5 -37.5°C) using a rectal thermometer interfaced with a servo-controlled heat lamp. Mice were anesthetized with 2% isoflurane, maintained under anesthesia with 1.5% isoflurane. The chest was shaved and the mouse was placed chest up on an examination board interfaced with the Vevo 770. The 707-B (30 MHZ) scan head was used to obtain 2D images of the parasternal long axis. M-modes were taken from the same anatomical position. The probe was then rotated to acquire a short axis view of the heart. Stroke volume (SV) was calculated as: Diastolic Volume-Systolic Volume. Ejection fraction was calculated as (SV/Diastolic Volume) *100%. Cardiac output was determined by: SV*HR. All images were acquired with the Vevo 770's rail system to maintain probe placement and allow for precise adjustments of position. Left ventricular diameters during diastole (LVIDd) and left ventricular diameter during systole (LVIDs) and heart rate (HR) were determined from long axis M-modes. Left ventricular fractional shortening (%FS) was calculated as ((LVIDd-LVIDs)/LVIDd) *100%.

Figure S1. Histidyl dipeptide levels are enhanced in the carnosine synthase (ATPGD1-Tg) heart.

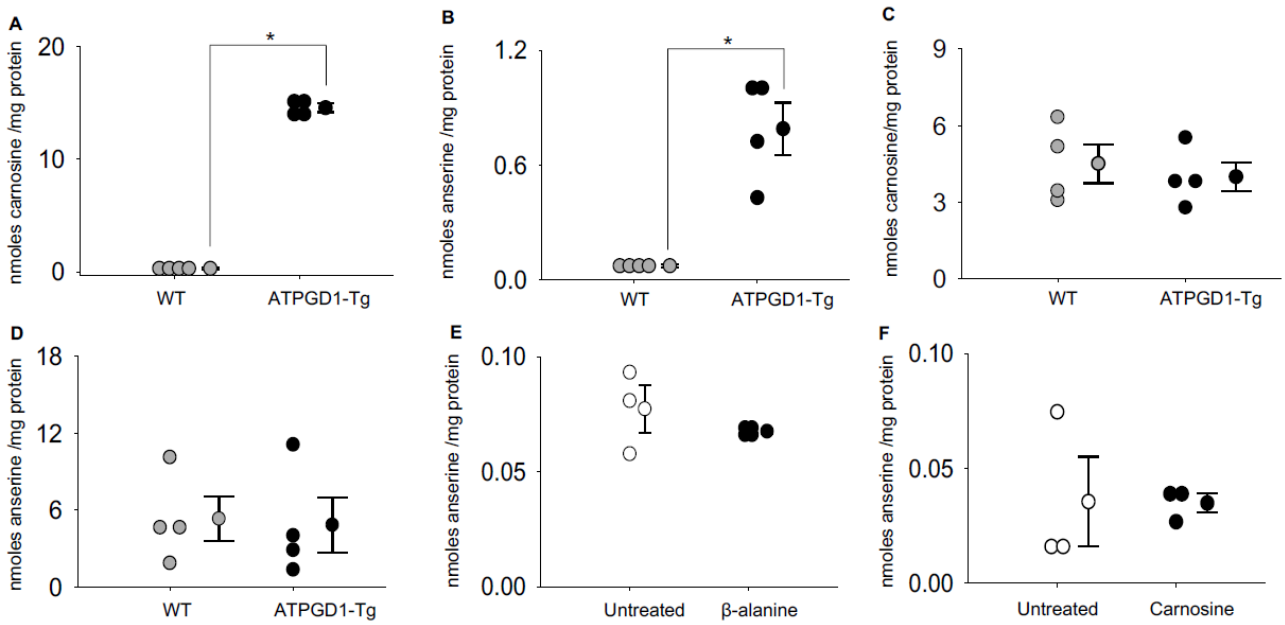

Levels of carnosine in the (**A**) heart and (**C**) gastrocnemius skeletal muscle of WT and ATPGD1-Tg mice. Levels of anserine in the (**B**) heart and (**D**) skeletal muscle of WT and ATPGD1-Tg mice. Levels of anserine in the hearts of (**E**) β-alanine and (**F**) carnosine fed mice. Data is presented as mean±SEM, n=4 mice in each group, *p<0.05 vs WT heart.

Figure S2. Synthesis of anserine.

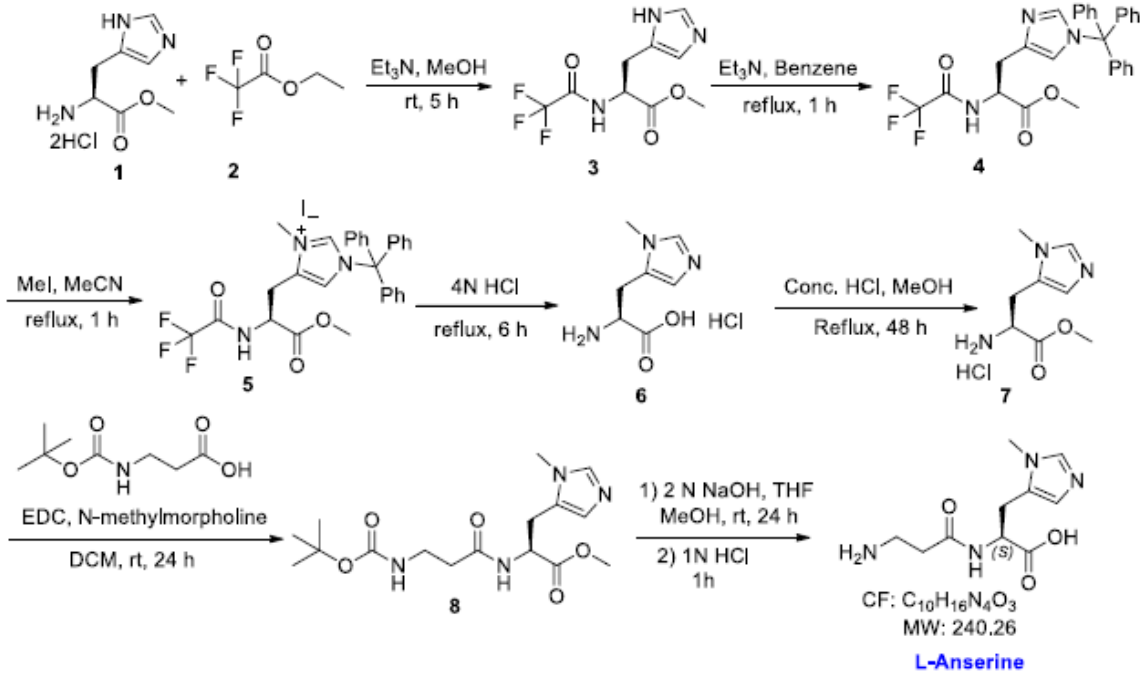

Table S1. Echocardiographic parameters of the wild type and ATPGD1-Tg hearts, age 12-14-week, n=7 in each group.

	Baseline	
	WT	**ATPGD1-Tg**
LVIDd(mm)	3.95±0.05	3.98±0.07
LVIDs(mm)	2.27±0.07	2.48±0.09
EF(%)	63±1	60±1
Heart rate	580±5	540±5
FS	41±1	38±2

Data are presented as S.D. in each group.